2021

# Characterization of Inhbb, Heatr5a, & Cyp2s1 Expression in Dorsal Root Ganglia by In-Situ Hybridization

Joshua D. Krech
*Wright State University*

# CHARACTERIZATION OF *Inhbb*, *Heatr5a*, & *Cyp2s1* EXPRESSION IN DORSAL ROOT GANGLIA BY IN-SITU HYBRIDIZATION

A thesis submitted in partial fulfillment of the

requirements for the degree of

Master of Science

By

JOSHUA D. KRECH

B.S., Ohio University, 2019

2021

Wright State University

WRIGHT STATE UNIVERSITY

GRADUATE SCHOOL

April 22, 2021

I HEREBY RECOMMEND THAT THE THESIS PREPARED UNDER MY SUPERVISION BY Joshua D Krech ENTITLED Characterization of *Inhbb*, *Heatr5a*, & *Cyp2s1* Expression in Dorsal Root Ganglia by In Situ Hybridization BE ACCEPTED IN PARTIAL FULFILLMENT OF THE REQUIREMENTS FOR THE DEGREE OF Master of Science.

David R. Ladle, Ph.D.
Thesis Director

Eric S. Bennett, Ph.D.
Department Chair
Department of Neuroscience, Cell Biology and Physiology

Committee on
Final Examination

David R. Ladle, Ph.D.

Patrick M. Sonner, Ph.D.

Mark M. Rich, M.D., Ph.D.

Barry Milligan, Ph.D.
Vice Provost for Academic Affairs
Dean of the Graduate School

# ABSTRACT

Krech, Joshua D. M.S. Department of Neuroscience, Cell Biology and Physiology, Wright State University, 2021. Characterization of *Inhbb*, *Heatr5a*, & *Cyp2s1* Expression in Dorsal Root Ganglia by In Situ Hybridization.

Multiple studies have shown that gene expression changes occur in sensory neurons after peripheral nerve injury (PNI). These expression changes include many genes that are turned on specifically in response to injury, but much less is know about expression changes in stable genetic markers of particular sensory neuron populations. This study characterized the expression of three markers of proprioceptive neurons *Inhbb, Heatr5a, Cyp2s1* in lumbar dorsal root ganglion (DRG) neurons in intact animals and after PNI. To perform these experiments, we subcloned segments of the coding sequences of these genes and generated DIG-labeled riboprobes. Control experiments demonstrated the validity of these probes for these genes on brain tissue from adult mice. Then we examined expression in the lumbar L4-L6 DRGs from adult mice that had undergone sciatic nerve transection or sham surgeries. Our results are preliminary but suggest that overall expression patterns did not change with each of the genes when comparing control and injured tissue. Nevertheless, further investigation is needed to make any conclusive results.

TABLE OF CONTENTS

LIST OF FIGURES

# I. Introduction

## *Proprioceptor Function*

Proprioceptors are a unique collection of sensory neurons which are used to detect the stretch, position, movement, and force of our muscular system. These proprioceptive sensory neurons (PSN) are directly related to coordination and proper movement of our extremities (Proske & Gandevia, 2012). The constant feedback from proprioceptive fibers provides the foundation needed to perceive a three-dimensional environment.

Proprioception is carried out by two separate mechanoreceptors, muscle spindle (MS) and Golgi tendon organ (GTO) afferent fibers. MSs are distinctive skeletal muscle fibers which are innervated by group Ia and group II afferents, which detect the length of stretch within a muscle (Wu et al., 2019). GTOs are located within the tendonous region of the muscle and are innervated by group Ib afferents, which detect tensile force (Wu et al., 2019). Together these mechanisms communicate vital information for the body's perception of movement.

## *Development of Proprioceptors*

MS and GTO neurons have cell bodies located in the dorsal root ganglion (DRG). The cell bodies store the genetic information in the nucleus which encodes for the functionality and morphology expressed by the neuron (Lallemend & Ernfors, 2012). Genetic information can be related to the functionality of the neuron by looking at the lineage and genetic markers during neurogenesis within the DRG. There are two genetic lineages with sensory neurons. These lineages can be divided into the Tkb+/Shox2+ and

TrkC+/Rx3+ gene lines (Kramer et al., 2006; Lallemend & Ernfors, 2012; Levanon et al., 2002; Ma et al., 1999). The TkB+/Shox2+ lineage consists of the Meissner and Pacinian Corpuscle sensory afferents which are responsible for light tactile touch and deep pressure sensation. Together these afferents are classified as rapidly adapting- low threshold mechanoreceptors (RA-LTMR) (Levanon et al., 2002). The TrkC+/Rx3+ lineage consists of the Merkel cells and PSNs like the GTOs and MSs mentioned above. Merkel cells are responsible for the shape and form of objects felt, and PSNs are previously mentioned to be subdivided into GTO and MS functions (Levanon et al., 2002). These are classified as slow adapting-low threshold mechanoreceptors (SA-LTMRs). Additionally, SA-LTMR that are TrkC+/Rx3+ and show expression of parvalbumin (PV+) are further defined as special mechanoreceptors called proprioceptors. This differentiates them from other SA-LTMRs which are PV negative (Levanon et al., 2002; Wu et al., 2019).

During embryogenesis proprioceptors are further differentiated into MS and GTOs by genetic markers that are expressed in this cell lineage beginning at embryonic day e12.5 in mice. Intrinsic transcription factors and extrinsic receptor sensory factors play a vital role in differentiating expression in stages throughout development. Proprioceptors reach their peripheral targets through day e17.5 (Wu et al., 2019). These genetic markers are classified as early, late, and transient markers depending on the stage at which they are first expressed during embryogenic development. Early markers are expressed from e12.5 and before the PSNs have reached their peripheral nerve endings, transient markers are expressed during innervation around e14.5, and the late markers are expressed after e17.5 and even during post-natal development (Wu et al., 2019). In this

study, we will focus on three genes: *Inhbb*, *Heatr5a*, and *Cyp2s1* which are classified as late markers and compare their expression in relation to peripheral nerve injury.

### *Peripheral Nerve Injury*

In this study we must define what peripheral nerve injury (PNI) entails. We are focusing on specific PNIs induced by kinetic energy. Peripheral injuries induced by kinetic energy can be classified as penetrating trauma wounds (Robinson, 2000). These can occur by several means such as work-related injuries, falls, gun-shot wounds, or any other incident with traumatic penetrating trauma (Noble et al., 1998; Kouyoumdjian, 2006; Missios et al., 2014; Kouyoumdjian et al., 2017). PNIs can go undiagnosed for several days due to other serious injuries needing more immediate attention (Noble et al, 1998; Robinson, 2000). PNI which are specifically induced by kinetic energy have been reported in about 1% of motor vehicle accidents and in 2% of patients in level 1 trauma centers (Noble et al, 1998). In this study we are excluding PNIs which are induced by chemical, hypoxic, thermal, or any diseased state which may cause nerve degeneration.

### *Mechanisms of Peripheral Nerve Injury*

Peripheral nerve injuries can result in considerable neuronal damage and create loss of motor and sensory function (Navarro et al., 2007). PNIs can be broken into several stages. First is the acute injury which occurs during the onset of the trauma. During the acute injury stage where the axon is severed there is an immediate influx of extracellular sodium and calcium cations (Ziv and Spira, 1993). The positively charged sodium and calcium creates high frequency signals inducing action potentials that make their way to the neuron cell body. These high frequency signals inform the soma that the plasma

membrane is damaged by the induced trauma (Navarro et al., 2007; Raivich and Makwana, 2007). Schwann cells covering the axon are also damaged and send intracellular signals up the axon in a retrograde fashion back to the soma of the neuron. This retrograde transport of intracellular components from the Schwann cell is believed to initiate the degeneration of the axon (Ziv and Spira, 1993; George et al., 1995). The degeneration of the axon is believed to begin around 24-48 hours after onset of the injury in rodents (Tsao et al., 1999). Humans on the other hand take much longer and this depends on the location of the injury in relation to the soma. Depending on the location of the injury whether proximally or distally to the soma, axon degeneration in humans can be delayed up to 7 days after injury (Chaudhry & Cornblath, 1992).

Initially Schwann cells will produce macrophages which release cytokines that act as pro-inflammatory mechanisms. Eventually these macrophages will then release anti-inflammatory cytokines which promote the healing and regeneration process (Gaudet et al., 2011; Chen et al., 2015). These macrophages clean up necrotic tissue and debris around the area of the injury during the first week of recovery in humans (Gaudet et al., 2011) The Schwann cells also produce neurotrophins which promotes neuronal survival and regeneration (Scheib and Höke, 2013). The neurotrophins do this by retrogradely traveling up the axon to the soma and promote phosphorylation cascades. These phosphorylation cascades will alter expression patterns of up to 60 proteins (Komori et al., 2007). Cellular debris and axonal injured tissue leftover will produce an increase in fatty acids. This will down-regulate some of these proteins involved with lipid biosynthesis. Some proteins will be upregulated like antioxidant and metabolic proteins because they will protect the injured neuron from oxidative degradation (Fu and Gordon,

1997; Komori et al., 2007). Overall, the acute phase of PNIs consists of the onset of injury, inflammatory response, neuronal repair, and survival. However, after the immune response subsides the healing and regeneration phase can be prolonged for months after the initial injury (Gaudet et al., 2011; Chen et al., 2015).

***Peripheral Nerve Regeneration***

During the regeneration phase of the axon, there is time sensitive interactions needed for reinnervation, this is known as the regrowth phase (Fu and Gordon, 1997; Komori et al., 2007) Significant reinnervation of axons to target tissues in humans are known to last between 10-12 months, compared to 35 days in adult mice (Ma et al., 2011). This time sensitive regrowth phase must occur before the degradation of the basal lamina in Schwann cells, loss of innervation causing muscle atrophy, and prior to an increase in the growth-inhibiting chondroitin sulfate proteoglycans (Zuo et al., 1998; Scheib and Höke, 2013).

Due to the time sensitive nature of the regrowth phase, studies have focused on increasing the growth rate which is between 1-3mm/day (Sunderland, 1947; Verdú and Navarro, 1997). Current studies focus on electrical stimulation and exercise. These studies have shown to help accelerate the regeneration of motor and sensory fibers (Elzinga et al., 2015; Gordon and English, 2016). However, patients still exhibited some disability and motor deficits even though axon regrowth was accelerated (Wong et al., 2015). The plasticity helps with gross motor components but the effect on fine motor skills is maladaptive, leading to neuropathy and other issues (Navarro et al., 2007). Studies also show that smaller diameter axons grow faster and more efficiently (Kang and Lichtman, 2013). These small-diameter axons include free-nerve endings in the skin

which are responsible for tactile sensation. As these smaller diameter afferents reinnervate with their nerve endings they simultaneously regain function (Verdú and Navarro, 1997). Compared to the larger diameter axons, which include the MS and GTOs, these smaller diameter afferents do not have specific targets. This is believed to be the reason why functionality is not fully gained in larger diameter axons because of their requirement to contact unique nerve ending targets to successfully transduce the appropriate sensory signals (Verdú and Navarro, 1997; Vogelaar et al., 2004).

When studying sciatic nerve crush injuries in adult mice, many large diameter afferents took up to 21 days after the injury to reinnervate plantar muscles in the distal foot (Verdú and Navarro, 1997). Although, even after axons reached their end point, axon projection density can increase for more than an additional 20 days. This means that it takes several weeks for specialized organs such as MS and GTOs to reinnervate with their end targets, which indicates that full regrowth of these afferents can extend beyond the critical period (Verdú and Navarro, 1997; Ma et al., 2011). Importantly, extra recovery time did not show any increased functional gains beyond those obtained during the critical period (Wang et al., 2015).

Focusing on the positive aspects of peripheral neuronal regeneration and limiting negative effects is an ongoing endeavor, and "an important direction for ongoing research is the development of therapeutic strategies that enhance axonal regeneration, promote selective target reinnervation, but are also able to modulate central nervous system reorganization, amplifying those positive adaptive changes that help to improve functional recovery but also diminishing undesirable consequences." (Navarro et al.,

2007). Reviewing mechanisms like the monosynaptic reflex will provide better understanding of the role's proprioceptors play in addition to their sensory inputs.

### *Monosynaptic Reflex*

The proprioceptive feedback mechanism communicates in multiple ways with our central nervous system. Mentioned previously were ways in which these sensory fibers convey ongoing stimulus to help with the bodies sense in space as well as balance and posture (Zimny, 1988). An important element of this sensation is the monosynaptic reflex. When the muscle is stretched, MSs are activated and send sensory information back to the spinal cord. Here the neuron immediately synapses with the motor neuron soma and stimulates an action potential from the excitatory stimulus. This generates contraction of the same muscle that was stretched. At the same time, the sensory neuron synapses with an inhibitory interneuron within the spinal cord that synapses with the motor neuron innervating the muscles antagonistic action at the same joint, relaxing these muscles. So, the overall effect of MS stimulation is to contract the same muscle that was stretched while relaxing the muscle in opposition to it simultaneously. This process happens very fast, on the order of 10s of milliseconds since the signal does not travel up to the brain before the motor response.

In peripheral nerve regeneration studies, the monosynaptic reflex has shown to fail to return to normal once the PNI and regeneration phase has occurred. This occurs even though the sensory and motor neurons reinnervate their ending targets (Bullinger et al., 2011; Prather et al., 2011; Verdú & Navarro, 1997; Wang et al., 2015). The PNI causes a reduction of synapses from the proprioceptive sensory afferents onto motor neurons within the spinal cord resulting in perpetual alterations of the monosynaptic

reflex function (Schultz et al., 2017; Bullinger et al., 2011). However, reflex abnormalities still exist when the circuitry abnormalities are controlled for (Vincent et al., 2015).

### *Transection vs Crush Peripheral Nerve Injury Studies*

Major differences between transection and crush procedures affect the outcome of the peripheral nerve recovery. During crush injuries the axon and basal lamina are still intact, and the neurons are still capable of following the same path back to the receptor end points (Hyde & Scott, 1983; Robinson, 2000). However, during transection injuries the axons and basal lamina are severed. This leaves neurons more vulnerable to innervating the inappropriate end receptors during reinnervation (Banks & Barker, 1989; Collins et al., 1986) Reviewing these studies can possibly lead to understanding the abnormalities observed with the monosynaptic reflex after peripheral nerve injury (Prather et al., 2011).

Studies have shown that neurons with non-specific binding during reinnervation tend to show physiological characteristics of the new receptors they innervate (Collins et al., 1986). So, neurons that originally innervate GTOs, could reinnervate with a new receptor ending that performs a different function. Meaning if the original GTO neuron reinnervates a MS fiber, that neuron will act as a MS sensory afferent and send information regarding muscle stretch (Banks & Barker, 1989; Collins et al., 1986).

Once non-specific binding occurs during reinnervation, the monosynaptic reflex shows abnormalities causing incorrect feedback signals within the spinal cord (Pierrot-Deseilligny et al., 1981). The original synapse is retained within the spinal cord, but with

new peripheral innervation to a different nerve ending, the monosynaptic reflex fails (Prather et al., 2011). Performing peripheral nerve crush injuries and observing the regeneration results, showing monosynaptic abnormalities, indicated that there was more occurring than just non-specific binding caused by transection (Prather et al., 2011).

Intrinsic factors of PNIs have not been studied in relation to proprioceptor regeneration. Perhaps some combination of altered intrinsic factors could explain why the monosynaptic reflex is lost even if the axon and basal lamina are intact. Reviewing specific genes that are present during peripheral nerve crush injuries could reveal more mechanisms occurring that are not yet known. Genes that are expressed in the adult mouse could be down or upregulated after PNI and could result in changes to the neuron function. Comparing the different types of proprioceptor genes mentioned earlier including the early, transient, and late markers in relation to these PNIs would give insight to the intrinsic factors expressed. This study is focused on the late markers that are shown to be expressed during embryonic day e17.5 and occur post-natal, which includes genes Inhbb, Heatr5a, and Cyp2s1 (Wu et al., 2019).

In order to study the expression of these factors, we began by cloning and creating an anti-sense RNA probe which would detect *Inhbb, Heatr5a* and *Cyp2s1* expression patterns within the L4-L6 lumbar DRGs and brain. By creating these anti-sense RNA probes, we could compare the difference in expression pattern between adult wild type mice and mice who underwent sciatic nerve transection surgery. We observed these expression pattern differences by using in-situ hybridization techniques. Observing these differences, we aspired to understand the intrinsic factors related to PNIs.

## II. Materials & Methods

### *Animals*

The experiments performed on all animals abided by the guidelines created by the National Institute of Health and approved by the Institutional Animal Care and Use Committee at Wright State University. In this study, seven wild type mice (52.A-F & 9.A) were used. These mice were euthanized on postnatal day 93, in preparation for in-situ hybridization. This was to test for the anti-sense RNA probes *Inhbb, Heatr5a, and Cyp2s1*. Two of the mice (52.A,52. F) underwent sham surgery consisting of the exposal of the sciatic nerve without sciatic nerve damage. Four of the mice (52.B-E) underwent sciatic nerve transection surgery. All mice were between 12-13 weeks old during the time of surgery. These surgeries consisted of exposing and in the case of the transected mice severing the left sciatic nerve. The mice were given 10 days to recover prior to euthanasia and collection of tissue. One of the mice (9.A) did not undergo transection or sham surgery but instead was used as a control showing the expression of the anti-sense RNA probes in the brain tissue using in-situ hybridization.

### *Tissue Samples*

After euthanasia, the mice were fixed in 4% paraformaldehyde (PFA). Dissection was performed exposing the vertebral column away from the rest of the body. The tissue was then stored in PFA for 24 hours, washed with PBS 3 times for 5-minute intervals, and then stored in 30% sucrose overnight. Dissection of the L4, L5, and L6 lumbar DRGs were then performed from a posterior approach. These DRGs were then frozen in a

mounting compound in a -80°C freezer until ready for the cryostat. The samples were cut using the cryostat at 16 μm thickness and placed onto individual slides. The slides were then stored at -80°C until ready for in-situ hybridization. Control tissue consisted of the parallel DRGs associated with the L4, L5, and L6 DRGs on the right side, since the left side underwent the transection or sham surgery.

***Creating RNA Probes***

Anti-sense RNA probes were created using subclones from full length cDNA. Novel primers were used to amplify between 500-900 base pairs unique to the specific cDNA sequences. Some of the primer sequences were taken from Wu, et al. (2019). Primer sequences consisted of: *Inhbb*- CCCTGACTTGTCCCAGGTTC forward primer, and TACGTGTGTCCAGAAGTGGC reverse primer; *Heatr5a*-GACGGAGCACAAGAACCTGA forward primer, and CAGATTGGGCCTCGGTACTC reverse primer; *Cyp2s1*-ATTCACCCTGCTCGCTCTAC forward primer, and ACGCTTCCAAACCTCAGGTC reverse primer. Polymerase chain reaction (PCR) experiments were performed using these primers to amplify the unique region on the cDNA. PCR products were then ligated with TA-cloning pCR™II Vectors. PCR results were confirmed with gel electrophoresis on 1% agarose gel and compared to a 100 base pair ladder. The subcloned plasmid was then transformed using competent cells and grown on an Ampicillin plate. White colonies were selected and grown up using LB broth and Kanamycin in a liquid culture. The liquid cultures were spun down and used to create a purified plasmid by miniprep. The purified plasmid was confirmed using gel electrophoresis on a 1% agarose gel and compared to a 1Kb ladder. Orientation was confirmed using genetic sequencing (GeneWiz). The

subcloned plasmid was then linearized, this was also confirmed using gel electrophoresis on a 1% agarose gel and compared to a 1Kb ladder. In the process of linearization, the subcloned plasmid was purified by using phenol/chloroform/isoamyl alcohol extraction.

Lastly, the linearized subclone was used to create a digoxigenin-labeled riboprobe by using SP6/T7 DIG labeling mixture. This DIG labeled probe was confirmed using gel electrophoresis and compared to a 100 base pair ladder. Concentrations and purity of all products were recorded using a spectrophotometric Nanodrop Machine (Thermo Scientific). The final riboprobes were used during in-situ hybridization experiments to show expression of specific genes (*Inhbb, Heatr5a, and Cyp2s1*) after PNI.

***In-Situ Hybridization***

In-situ hybridization experimentation was used to show the expression of proprioceptive genes *Inhbb*, *Heatr5a*, and *Cyp2s1* in PNI and control mice tissue. Digoxigenin-labeled riboprobes previously mentioned were used to reveal gene expression. The protocol is a 3-day process and is outlined below.

***Day 1:*** Tissue sections were thawed at room temperature. While the tissue was thawing, solutions were made for the various washing cycles. The slides were washed in a series of solutions including 4% paraformaldehyde, PBS, proteinase K, an Acetyl buffer, and formamide to prepare for the DIG labeled probes. After formamide solution was added and the slides were left to sit for an hour. A hybridization buffer was made which consisted of formamide, 20x SSC, 50x Denhardts, yeast RNA, salmon sperm DNA, molecular biology grade water, and unique DIG labeled probe. After the hour wait time,

the solution was dumped off and the hybridization buffer was added. A cover slip was added, and the slides were left to incubate overnight at 65°C.

***Day 2:*** After overnight incubation slides were washed with preheated 5x SSC to remove cover slips and then set to incubate in 0.2x SSC at 65°C for one hour. Slides were then washed in PBST. A solution of 10% normal goat serum was made and added to the slides to incubate at room temperature for one hour. Then, a solution of 1% normal goat serum and anti-DIG antibody in PBST was added. The slides were then stored in a moist chamber at 4°C fridge overnight.

***Day 3:*** The slides were rinsed with a series of washes with PBST and B3. A developing solution was made by adding B3 and developing reagents. This developing solution is light sensitive and was kept in the dark by enclosing the tube containing the solution with foil. Once the developing solution was added to the slides, the plastic chambers were also encased with foil. The slides were examined every hour under a microscope until expression was shown. Some slides received an additional dose of developing solution and were stored in the 4°C fridge overnight. Once slides were done developing, they were heated at 55°C to dry and Dako glycergel mounting medium was added to preserve them.

### *Analysis*

The gene expression patterns were examined using a brightfield Olympus BX51 microscope. CellSens software was used to capture and observe images of the DRGs from the slides. Each DRG was imaged using 4x and 10x lenses and labeled accordingly. Images were analyzed using ImageJ software and specific rainbow expression pattern images were collected using unique Allen brain atlas look up tables (LUT) (Allen, 2007).

DRGs were analyzed for specific gene expression patterns by counting the number of cells showing positive expression and dividing by the total area of each DRG. To calculate the specific area of each DRG, the ImageJ software was used and set to scale by measuring the 100 μm scale created by the CellSens software used to image the DRGs. Positive expression was determined by significant dark purple staining cells. Only the L5 images of the DRGs from each animal were used for analyzation because in previous findings the L5 DRG contains the majority of proprioceptive cells from the sciatic nerve.

## III. Results

### *Cloning*

The goals of this study consisted of creating anti-sense riboprobes that specifically identified the expression patterns of our genes in question (*Inhbb, Heatr5a, and Cyp2s1).* The gene sequences are shown in Figures 1, 2, & 3 and show the unique forward and reverse primers used additional to SP6 and T7. To accomplish the objective of our anti-sense riboprobe a subclone of these genes' DNA sequence was amplified using PCR. Results from the PCR amplification are conveyed in Figures 4, 9, and 14. Next, this amplified sequence was ligated using TA-cloning pCR™II vectors. A representation of the pCR™II vector is represented in a vector map from Figures 8, 13, and 18 indicating sequence orientation, location of primers, and enzymes used to linearize the plasmids. These plasmid vectors were then grown up on LB agar plates and X-Gal was added to transform any bacterial colony which did not contain the DNA inset to a blue colony. So, only white colonies were selected and grown in a liquid culture. A miniprep of the spun down liquid cultures was performed to purify the plasmid. Results in Figures 5, 10, and 15 show the expected base pair length of the purified plasmid, showing evidence that the plasmid correctly represents the specific gene sequence in question additional to the pCR™II vector. The plasmid vector was then linearized to allow for proper binding to DNA during in-situ experiments. The linearized plasmids are confirmed using gel electrophoresis and are represented in Figures 6, 11, and 16. Finally

a DIG labeling mixture and T7 polymerase was added to the *Inhbb* and *Heatr5a* linearized plasmids. Adding the T7 polymerase is specifically added due to the plasmid's orientation. For *Cyp2s1* a SP6 polymerase was used due to its reverse orientation. The final riboprobes are confirmed for base pair length using Gel electrophoresis and are shown on Figures 7, 12, and 17. *Inhbb* and *Heatr5a* showed expected base pair length when compared to a 100 BP Ladder. However, in Figure 17 *Cyp2s1* was expected to have a base pair length of 404 BP, but showed a base pair length between 700-800 BP. Again, the purified plasmid after the miniprep was sent for sequencing (GeneWiz). So, our results for the *Cyp2s1* riboprobe were inconclusive. Nevertheless, we knew our gene specific sequence was still within that base pair length, and due to time constriction, we decided to move on to the In-situ hybridization stage to confirm the validity of our riboprobes.

***Control Tissue***

Our first goal of confirming our DIG labeled riboprobes worked was conveyed through using the control brain tissue of 93-day-old mice (9.A). This showed expression patterns of our specific genes throughout the brain. Sagittal sections of the brain were viewed throughout various regions of the brain including but not limited to the cortex, cerebellum, hippocampus, and olfactory bulb. After In-situ hybridization the brain tissue was imaged and analyzed. These images were compared to images taken from In-situ hybridization experiments performed by the Allen Brain Institute which are represented in Figures 19, 21, and 23 (Allen, 2007). Expression patterns unique to each gene were examined and carefully compared to the Allen Brain Atlas (ABA) images. The *Inhbb* riboprobe in both the control shown in Figure 20 and ABA tissue (Figure 19) showed

high expression in the cerebellum, olfactory bulb, cortex, and the hippocampus. This is different to the expression patterns shown in Figures 22 and 24 (*Heatr5a* and *Cyp2s1* respectively). *Heatr5a* (Figure 22) and ABA tissue (Figure 21) showed high expression in the cerebellum, cortex, and olfactory bulb but not in the hippocampus. While *Cyp2s1* (Figure 24) and ABA tissue (Figure 23) mainly showed expression in the cerebellum and cortex.

Separate from our control brain tissue, we used sham surgery injured animals as a control. As stated previously, sham animals undergo sciatic nerve exposure surgery, but no damage is done to the sciatic nerve. Additional to the sham animals, only the left sciatic nerve was transected in each injured animal, meaning that the right side of that animal provided an additional internal control. So, along with the sham animals (52.A/52.F) the parallel right DRGs were used as controls to the left DRGs on the injured side. Lastly, expression of *Parvalbumin,* a known marker of proprioceptive neurons, was used as an additional control as its expression is known to remain stable after peripheral nerve injury (Wu et al., 2019).

In Figures 25, 27, 29, and 31 (*Inhbb, Heatr5a, Cyp2s1, and PValb respectively)* shows the results from comparing the number of genes expressed (dark staining) over the area of the total DRG in $\mu m^2$. These figures showed the relationship between the sham injury animals and the transection-injured animals right L5 DRGs (nonaffected side). Based on the data in these figures we observed no change in expression in our control tissues with all our genes. Lastly, in Figures 33, 35, 37, and 39 expression of our genes were compared in the sham animals (52.A/52.F) between the right and left DRGs. Additional to the In-situ results, these images were rendered with the Allen Brain Atlas

look up tables to better represent the effects of the expression patterns. Reviewing the figures below some DRGs show greater expression than others, but as stated previously comparing the sham animals, there was no difference in the average expression numbers when divided by the total area of DRGs in $\mu m^2$.

### *Transection-Injured Tissue*

Once we confirmed that our DIG labeled riboprobes worked, our next goal was to see if there was any change in expression between our control DRGs and the transection-injured tissue. Our general assumption was that since *Inhbb, Heatr5a,* and *Cyp2s1* are late markers (expressed post-natal), expression would be down-regulated 10 days after surgery when the tissue was collected.

When observing Figures 26, 28, 30, and 32 we can see the expression patterns compared to the sham animals (52.A/52.F). This was data collected from the left L5 DRGs from each transection-injured animal and the two sham surgery animals. Expression patterns showed no change when compared to the sham animal controls. In Figures 34, 36, 38, and 40 the transection-injured animals right vs left L5 DRGs were compared. Although, expression was shown in each DRG, as stated previously no significant change in expression was observed.

*Inhbb* cDNA Sequence (BP:1-3054)

```
ORIGIN

   1 cccggagctc cgggtggctc gcaggacacc tgtacgtcgt gcggcggcgg cggcggcggc
  61 ttccggcggc cggaggagct gggccgggtg gacggtgact tcctggaggc ggtgaagaga
 121 cacatcttga gccgcctgca gttgcggggc cggcccaaca tcacgcacgc tgtccccaag
 181 gccgccatgg tcacggccct gcgcaagctg cacgccggca aggtgcgcga ggacggccgc
 241 gtggagatcc cgcacctcga cggccacgcc agcccgggcg ccgacggcca ggagcgcgtc
 301 tccgagatca tcagctttgc agagacagat ggcctcgcct cctcccgggt ccgcctgtac
 361 ttcttcgtct ctaatgaagg caaccagaac ctattcgtgg tgcaggccag cctgtggctg
 421 tacctgaaac tgctccccta tgtcctggag aagggcagca ggaggaaggt acgggtcaag
 481 gtgtacttcc aagaacaggg tcacggagac aggtggaatg tggtggagaa gaaggtggac
 541 ctgaaacgta gcggctggca tacctttccc atcacagagg ccatccaggc cttgtttgag
 601 cgaggcgaga gacgccttaa cctggatgtg cagtgtgaca gctgccagga gctggccgtg
 661 gtgcctgtgt tcgtggaccc cggtgaggag tcacacaggc cctttgtagt ggtgcaggcc
 721 cgcctgggcg atagcagaca tcgcatccgc aaacggggcc tagagtgtga tgggcggacc
 781 agcctctgtt gcaggcaaca gttcttcatc gactttcggc tcatcggctg gaacgactgg
 841 atcattgcgc ccactggcta ctacgggaac tactgtgagg gcagctgccc ggcctatctg
 901 gccggggtcc ctggctcagc ttcctccttc cacacagccg tggtgaacca gtaccgcatg
 961 cgtggcctga accctgggcc cgtgaactct tgctgcatcc ctaccaagct gagctccatg
1021 tccatgctct actttgatga cgagtacaac attgtcaagc gggatgtacc caacatgatc
1081 gtggaggagt gtggctgcgc ctgacagagg caacgggggc ggagcacagg cccatgggtc
1141 tttgagggag caggagaggc aggtgggctg agtgtggttg ttccattggg ccgtgaagag
1201 tgccagggtg aggcctgaaa taatgttctc ccgctttgta gaaaaccagt caggaccaga
1261 gggagaatcc ctctgtgaca cgagagactc ctaactgcac acatagacac gcatagccag
1321 actcacgcag tctgccaccc acacagcagc ctctgggata ccagcaaacg gatgcggtga
1381 caaatggcac caatgcctgt cagtctgaaa gaatggggtg agcagccacc attcccacca
1441 gctggccggg cactctgaat tgcgccttct gagcacacat aaaagcacac aaagacagag
1501 gacacagaga gagtgagcca gagagccacc aagaggaaaa gcagggtggg agcacaggcg
1561 ggtggagggc catgtgtccc tgacttgtcc caggttcttc accgaagcgc ctggcacagt
1621 cctgcctgct cactgcccgc ctggcatcct ccatgctttg aggccagcag agctgtgcca
1681 cccctgttct tggagagggc aagtagccca ggagggactc acctgtcaca gagaccatgg
1741 agcagggaca gtgacccttt gatggtctgt cacttgcgtc ccccatgtga cttatatatg
1801 tgtgtatgtg tgtttgtttt cgggggtgtt gggggaggga gagaagaagg gtcttaattt
1861 tatgctttaa attcatctcc aacaactgac aggtcactgg tgccagttgc agaattgaaa
1921 agagcctatc agctatggcc tttgaagcgg aaaggccaaa cgattcgaag tgagaaggaa
1981 agaaaatgtt gcaatcggtg ccctttgctg gggacttcct cctggtgtta tgcttagagg
2041 ggagggccac tggcaaggga gagagacagg ggaggcagtg gcagagtgag gctgttctga
2101 ggagctgctc agctgggctt ggagagagag ggagagcttt tggttgcttt gcagaagttg
2161 tccccgaggg tgagccctgg cttcagggtt gtccgtggac atgtcccctg cccagttcac
2221 ttgccctccc gcctgctcca caatgcactt gcggtcctga gtgaatgcac accacaatag
2281 cacttgcagg tctacgtgtg tccagaagtg gcctggggc gagagcttga cgtggctgtc
2341 ctcgtggatg tccaagtgcc acgtgaacta tgcaatttaa agggttgacc cacactaggc
2401 gaaactggac tcgtacgact cttttatatt tttatacttg aaatgaaatc ttttgcttct
2461 tttctaagcg aatgattgct ttcaatgttt gcactgatct agttgcatgg ttagtcagaa
2521 actgccattt gaaaaaaaag ttatttttat agctgcagaa aaatgaatac agttaaatgt
2581 attatacata attttggaac caaagaggcc agcggatcag ttttaatttt tattagatgg
2641 tgaggccatc ttctatgagg tagatgttct aaacaatcct ttgagtggcc tgccagtgtt
2701 tcagggtata aatgattttt tttttattca gttgatgtgt cttttctgtc cgtacacacc
2761 cagaaggtag agtaaaataa atgactggtg gagtgaaggt gtgtgctgta agtcctcacc
2821 tttagtttat ttaataaatc cctccttagg ttctgtttca taataactta aaaccaaaca
2881 attttccccc acagactggc tgtcttaagt attttacgtt catgtacagt ttaagacaat
2941 aaaagatgga gtgccacggg caaaaaaaaa aaaaaaaaaa aaaaaaaaaa aaaaaaaaaa
3001 aaaaaaaaaa aaaaaaaaaa aaaaaaaaaa aaaaaaaaaa aaaaaaaaaa aaaa
```

**Figure 1.** Full *Inhbb* cDNA sequence map gathered from NCBI website. Original sample of cDNA sequence was from Dharmacon. Highlighted region represents subcloned section which was amplified using PCR. This consisted of 735 base pairs. The green highlighted represents the forward primer and the blue highlighted region the reverse primer.

*Heatr5a* cDNA Sequence (BP: 1-3793)

```
ORIGIN
        1 ggtgctccat cttgctgact tgatccgcat ggctttcatg gctgccacag accacagtga
       61 ccagctccgt ctctctggcc ttgacacact cttggtagtt atccgacggt ttgcagatat
      121 tgcagagcca gagtttccgg gtcatgtgat tctggaacag tatcaagcca atgttggagc
      181 cgctcttaga ccagccttca cttcagagac accacctgac atcaccgcca aagcatgtca
      241 ggtttgcagt gcttggatag caagtggggt tgttagtgac ctcagcgatc tccgcagagt
      301 tcatcagcta cttgtctctt ccctgacgaa gattcaggct ggaaaagaag ctctcagcca
      361 gctgtacaat gagagtgcct ccaccatgga gatcttagct gtgctgagag cctgggcaga
      421 ggtctatata attgctgtac aaagacataa aaatcacaag caagccttga agactactgt
      481 taattctgaa gacagtatga gaaacgggtc ctcttcagct gctggtcttc ttgacttagt
      541 ctgcactgac ctggccacgc taagcaaact ctggcttgct gcacttcagg attttgctct
      601 cttaactttg cctgcagaat ttgcttccca gcttcctact gaaggtggtg ctttctacac
      661 agcagagacg agcaagagtg caaagctaca ctaccacgac tcctgggccc tcatcctcca
      721 cgctgcggcc ctgtggctca ccagcacggg cttcgctgac ccagatgaag gcggtgccaa
      781 tctctcaagg cctgtaactc caacatccat gtgccagggc tcatcatcat caggagctgc
      841 cgtgaagtcc cccgaggatg tctacactga caggttccat ctgattctag gaatcagcgt
      901 ggagttcctg tgttccctgc gctcagatgc aagcttggaa agcatcatgg cttgtctgcg
      961 tgcactgcag gccctgctcg atgttccttg gcccaggtgg agaattggca gtgatcagga
     1021 cttgggtatt gaattgctaa atgtactaca ccgagtaatt ttgaccagag agtcaccagc
     1081 cattcaactg gcttcacttg aagtggtcag gcagattatc tgcgccgccc aagaacatgt
     1141 gaaggaaaaa agacgtagtg cagaagttga tgatggagcc tctgagaagg aaaccctgcc
     1201 agagtttggt gaagggaagg acacaggagg actcgtacct gggaagtctt tggtctttgc
     1261 aaccctggaa ctctgtgtct gcatcctcgt tagacagctc ccagaactga accctaagct
     1321 ggcaggtagc ccaggaggaa aggcttcaaa gccgaagacc ctgttggagg agggaagtag
     1381 actggtggcg gctgccctgg ccatccttgc tgagcttcct gcagtgtgct ctcctgaagg
     1441 cagcatctca attctcccta cagtattgta ccttaccatc ggagtcctcc gggaaacggc
     1501 tgtgaagtta cctgggggcc agttatcctg cacagtcacg gcttccctgc agactctgaa
     1561 aggaatctta acttccccca tggcccgggc agaaaagagc cacgaagctt ggaccagcct
     1621 cctccaaagt gcattagcaa ctgtgcttga ctgctggagc ccagttgacg gagcacaaga
     1681 acctgatgaa gtcagtctgc ttactgccgt cacagtattt attttgtcta ccagcccaga
     1741 agtgacaacc gtcccctgcc ttcagaatcg ctgcattgaa aaatttaagg ctgccctgga
     1801 gagcaaggac tctgtggtgc aaatgaagac ctgtcagctc ctccactcca tttttcagta
     1861 tccaaagccg gccgtttcct acccatacat ttattcctta gcatcttcta tcgtggagaa
     1921 gcttcaggac atagccagga ggaaacccga agatgctacc gagctgcagc tctgtcaaga
     1981 aggaataaag ctcttagaag ctttggtcgc cattgcggaa gaagagcacc gcgctcagct
     2041 ggtggcctgc cttctgccca tcctcatctc cttccttttg gatgagaatg ctctgggatc
     2101 agcaacttca gtaacgagaa gtctgcacga ctttgctttg cacagtctca tgcagattgg
     2161 gcctcggtac tcgtctgtgt ttaaaagagt catggcttct tccccagccc tgaaagcccg
     2221 gctggaggct gctgtaaaag gcaatcagga aagtgtccga gtggatccgc cttctaagca
     2281 tgccaagaac ctggccagga actccagcat ccagctaaag accaatttcc tgtgagctgc
     2341 tctcctagca cactgagcgc ctgaatgtaa cgcttggtgt ttccttgctt tggggacaaa
```

```
2401 agtggaactt gaggcacgag tgcacttgga gatcctgttg atcgttctca tttcaggagg
2461 gaccgaaact taacgttctt ggtaattctg gttttatttt gtttccattt actaagacca
2521 tggaactgtc aggattcttg ccaggcattt caagaaagtg ccaaagatcc aaatttacta
2581 agcaatccac tgctttgaaa atgaagggat gtcctctaac agtctgtatg tcctctaact
2641 gtctatcact gtattataaa gtatctgcgc ttacaccaca tcccactttc tacatggact
2701 cctgccttat tcagtggtcg tatcaaactg tgttgcattt ctcaagcaac atcaacaatt
2761 agagcagggg agggtggcac tcacctgagg agactgagac aggatgatca tcaaagttcc
2821 aaccagcctg gtctactgag tgagttccag accagctgtg accacacgat aggacttctc
2881 tcaaaaaata aattaacaaa ctaactaaca ataataatgc caacaataaa taagtgattg
2941 caacactctt taataactag acctaagcca ggctcatgcc tctaatccca tcactcagga
3001 gacaggcaag tggatctctg tgagttcaag gccagcctgg tctacagagt gagttccagg
3061 acagccaggg ctacacagag aaacctgtct caaacaaaga accaaatcta gaattaccca
3121 acttataaca ggagagacag cttcagcccc actgtgtggc ttgaggctgt ggtctcatga
3181 ttctgtcttt taagtgagtc tatgctgaga tcacgcagga tgcttttatg tagaatatag
3241 aacgatcacc ctcctaccat tctcagatgg attttctgtt acctctgttc cttttgtttt
3301 ggtttttat ttgtggaaat cattcatatt gaaagcttaa tatagagtca tgtctatatc
3361 gatttggggt tatatgaatg tcagatttag tacaacaaat ttagaacttc agtgaatacg
3421 aatacttttt taacacagaa tgtattttaa tataaaaata taatgataaa gtcatactgg
3481 tagaaaatat tttttggctg tttacgatca ttttccctcc acttcagtat tgttctgtgt
3541 gaattgacca ctgtgtcaga atgatgcagc ttcctgttaa aatttacaaa atgcagggac
3601 agaggtgtag ccagaattga gaaaaactga ttagaccaag agcacgtggt ggactctgtt
3661 ttattatgtt tgtatgtaaa tactcttgta aagcattcag agtggaaaac atttgacaaa
3721 ctctaacact aaaatcaact tttctacatt acataaataa agctaatttt ctttaaaaaa
3781 aaaaaaaaaa aaa
```

**Figure 2.** Full *Heatr5a* cDNA sequence map gathered from NCBI website. Original sample of cDNA sequence was from Dharmacon. Highlighted region represents subcloned section which was amplified using PCR. This consisted of 506 base pairs. The green highlighted represents the forward primer and the blue highlighted region the reverse primer.

*Cyp2s1* cDNA Sequence (BP: 1-2664)

```
ORIGIN
        1 cggcaaggag cttctaggag gtacagaccc agccgacctg cagagatgga ggcagccagc
       61 acctgggcgc tgctgctggc cctgctgctg ctgctgctgc tgctgtctct gacgctattc
      121 aggaccccgg cccgaggcta cctacccccg gggcccacgc cgctgccgtt gctggggaac
      181 ctcctgcagc tgcgtcccgg ggctctgtac tcggggcttt tgcggctaag taagaagtat
      241 gggcctgtgt tcacggtata cctgggcccc tggcgccgcg tggtggtcct ggttggacat
      301 gatgctgtaa gagaagcctt gggaggtcag gctgaggaat tcagcgggcg tggaacattg
      361 gcaacgctgg acaagacctt tgatggtcac ggagttttct ttgccaatgg ggagcggtgg
      421 aaacagctga ggaaattcac cctgctcgct ctacgggacc tgggcatggg caagcgagaa
      481 ggcgaggagc tgatccaggc ggaggtgcag agtctggtgg aggctttcca gaagacagaa
      541 ggacgtccat tcaacccttc catgctgctg gcccaggcca cctctaatgt cgtctgttcc
      601 cttgtcttgc atccgttt gccctatgac gataaagagt tccaggctgt gatccaggca
      661 gcaagtggta ccttgttagg gatcagctct ccatggggcc aggcctacga gatgttctcc
      721 tggctactgc agcccctgcc aggcccccac acacagctcc agcaccactt gggcaccctg
      781 gctgccttca ctatccagca ggtacagaaa caccagggac gcttccaaac ctcaggtcct
      841 gcacgtgatg tcgttgacgc cttcctgcta aagatggcac aggagaaaca agacccaggt
      901 acagaattca ccgagaagaa cttgctgatg acggtcacat acctgctgtt tgctgggacc
```

```
 961 atgaccatcg gtgccaccat ccgctatgcc ctcctgctcc tgctgagata ccctcaagtc
1021 cagcagcgcg tccgggagga gctcatacag gagctgggtc ctggcagggc tccaagtctc
1081 agcgatcgag ttcgcctccc ttacacggat gccgttttac acgaggcaca gcggctcctg
1141 gcactggtac ccatgggcat gccccacacc atcacgagga ccacttgctt ccgagggtac
1201 actctgccca agggcactga ggtcttccct ctgattggct ccatactgca tgaccctgcg
1261 gttttccaga acccaggaga gttccatcca ggccgcttcc tggacgaaga tggtcggttg
1321 agaaaacacg aagccttcct gccctactcc ttaggtaagc gagtctgcct gggagaaggc
1381 ctggctcggg cggagttgtg gcttttcttc acttccatct tgcaagcctt ctccctggag
1441 accccgtgcc cgccgggtga cctgagcctg aagccagcca tcagtggact tttcaacatc
1501 cccccggact tccagctgcg ggtctggccc actggcgacc agtccagatg aaggaaggag
1561 tttggaaggt gggagccctc tgggctgaaa gagccttact cagggtgtgt gtgaagcagg
1621 tgtctcagaa gcaacatcac actacacacc acgtatcaag gcagctgtgg agaccaggga
1681 ccacaccact acacaaccgc acagcaactg atgcataggc ttctttttgg agagggctgt
1741 ctgaaacggg gatcttgtta tgtggtgaca caagccgaac tcaaacttgt gatcctcccg
1801 cctcggtgtc ctgctcgctg gaattacagg tatgcgccac catgagctgc ataggctttc
1861 agcctacatc atgtaatata ggccatctgg aattgcaagc atatagctag ataccccgct
1921 gtccaccaca cgactctgta tgctcacaac tctaatccag cgactgccta cacaaacaca
1981 caaacaaccc aaccgtattc aggactctta actctgtcta acacgctcag caccgctgtt
2041 gctgggtccc cgccatagaa aacagcaagc cccagctggg gtcatgtcac agccagaacg
2101 atgttctgtc tactcccatg gatgacctca ccaccatcca ggctcatgag tggctctatc
2161 aacggccacc agccagtaat ccacacagcc aaaccgtatg tgacaagatc ttggcccttc
2221 caaacttctt cccactgagg cacaccgtga cgacatacta ttccccagtc acgtccacac
2281 ccatgccccc ccagcacgct ccttccaaca aatgttccca aatataaagg tttcctggtc
2341 tgtgattgtg cacacagacc ttctacaaat gaggaccagc gacccaaaga aaaagggttt
2401 cccagtcatg ttatcagggg cctgctctca aacgcattct gatctctgag ctgcctgcaa
2461 gtcctcatga gagtgctgga aatgtatcct cctcctggaa ggactaactg gcctcacagg
2521 gatgatgcag gggagtgctg ttagctgttt ccagccctcc ttatcaggac agaagccata
2581 gctgacctct ttgtgacttg aaggttcccg ttttgcaata aaagtttgtt tctggcccga
2641 aaaaaaaaaa aaaaaaaaaa aaaa
```

**Figure 3.** Full *Cyp2s1* cDNA sequence map gathered from NCBI website. Original sample of cDNA sequence was from Dharmacon. Highlighted region represents subcloned section which was amplified using PCR. This consisted of 404 base pairs. The green highlighted represents the forward primer and the blue highlighted region the reverse primer.

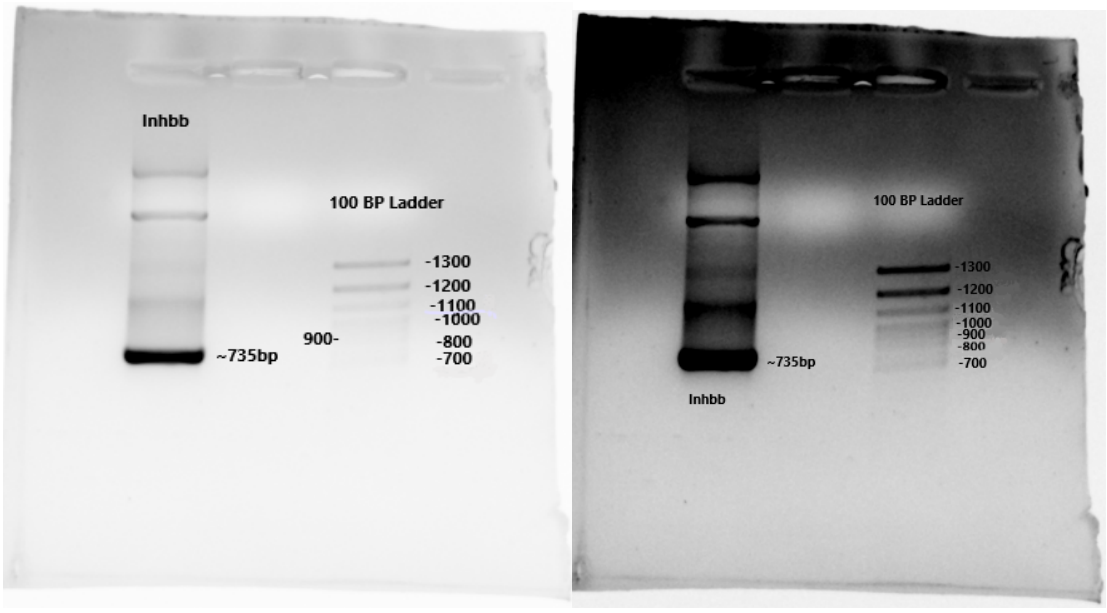


**Figure 4.** Gel electrophoresis product of *Inhbb* PCR sublcone compared to a 100 BP Ladder. Band size showed a positive result of 735 base pairs which confirmed our product was the correct sequence length. This PCR product was then ligated with TA-cloning pCR™II vector.

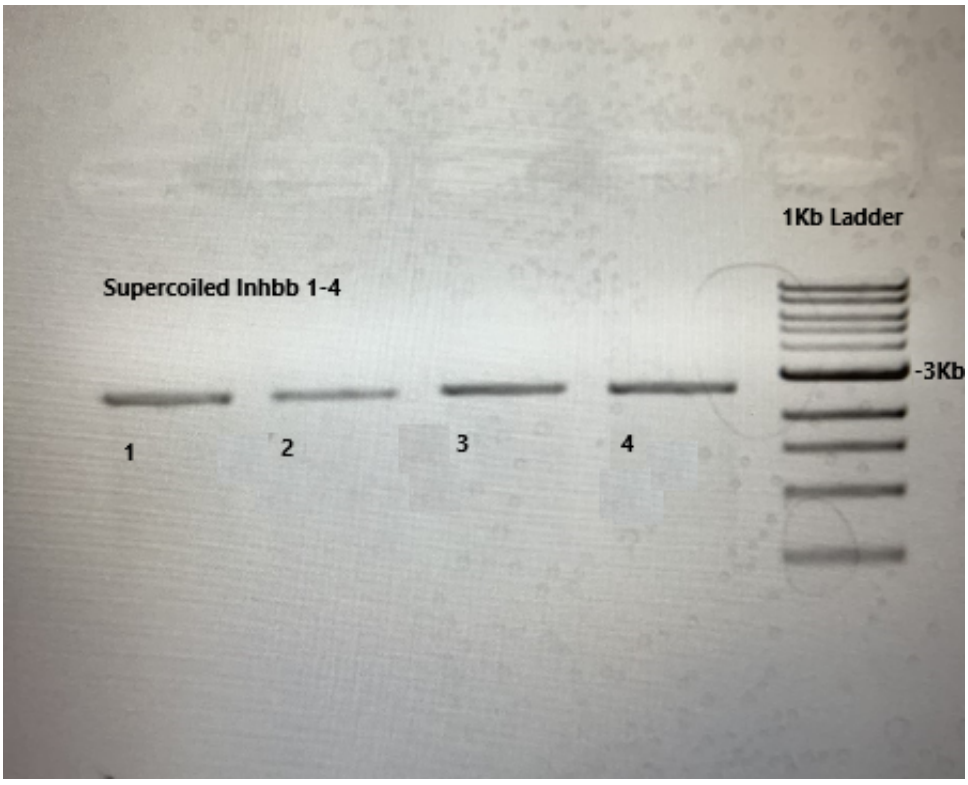


**Figure 5.** Gel electrophoresis product of *Inhbb* that has been grown up in a liquid culture and purified. The band length is compared to a 1Kb BP Ladder and is just under 3Kb BP in length which confirms our product is the correct length. This is considering the dark staining to be a supercoiled version of the plasmid vector. This product was sent off for sequencing (GeneWiz).

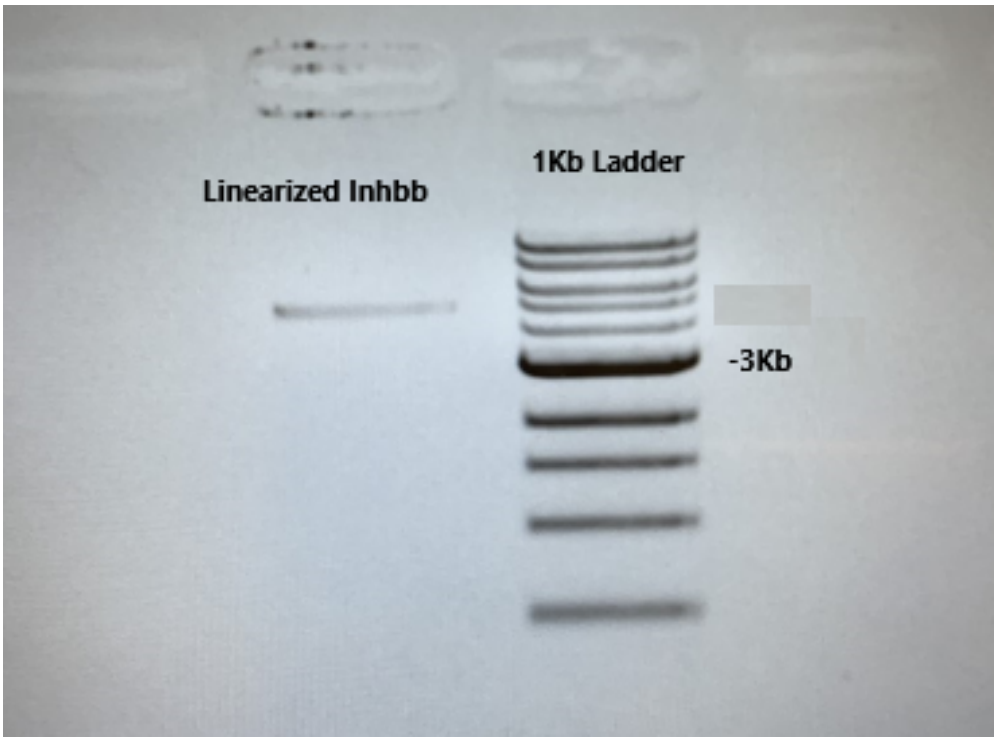


**Figure 6.** Gel electrophoresis product of purified *Inhbb* plasmid vector that has been linearized with BamH1. This product is compared with a 1Kb BP Ladder and confirms the phenol/chloroform/isoamyl alcohol extraction was succesful. This product was used to make the final riboprode product by adding a DIG labeling mixture to it.

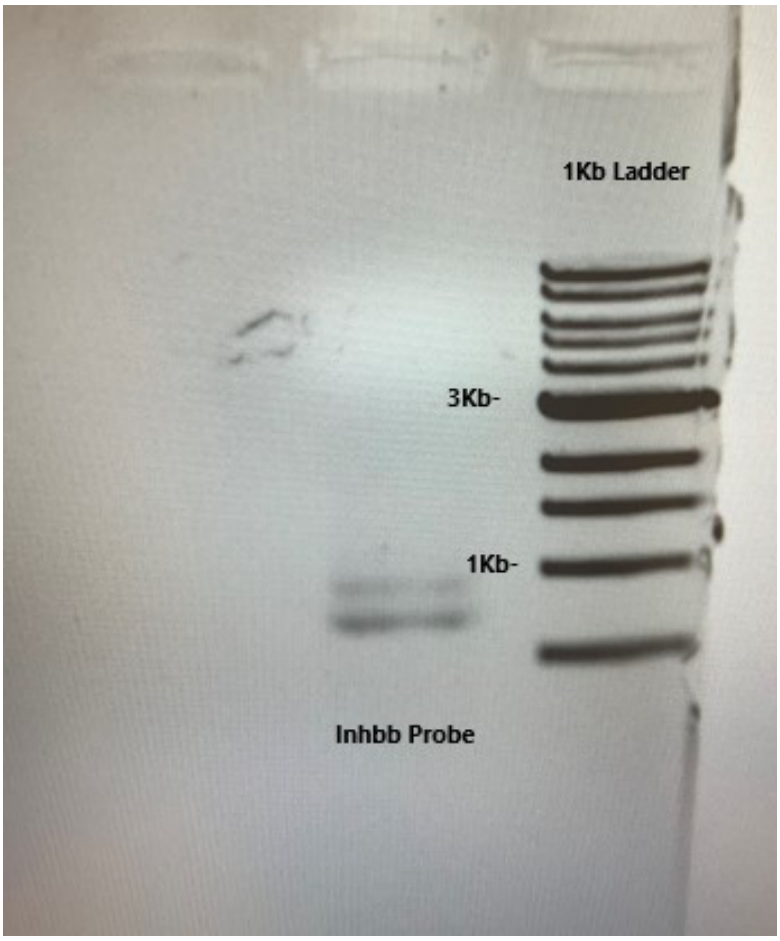


**Figure 7.** Gel electrophoresis product of *Inhbb* DIG labeled riboprobe compared to a 1Kb BP Ladder. The band size of 735 base pairs confirms that our sequence is of the right length. This product was used in our In-situ Hybridization experiments to show the expression of *Inhbb* in both the transection-injured and sham surgery mice.

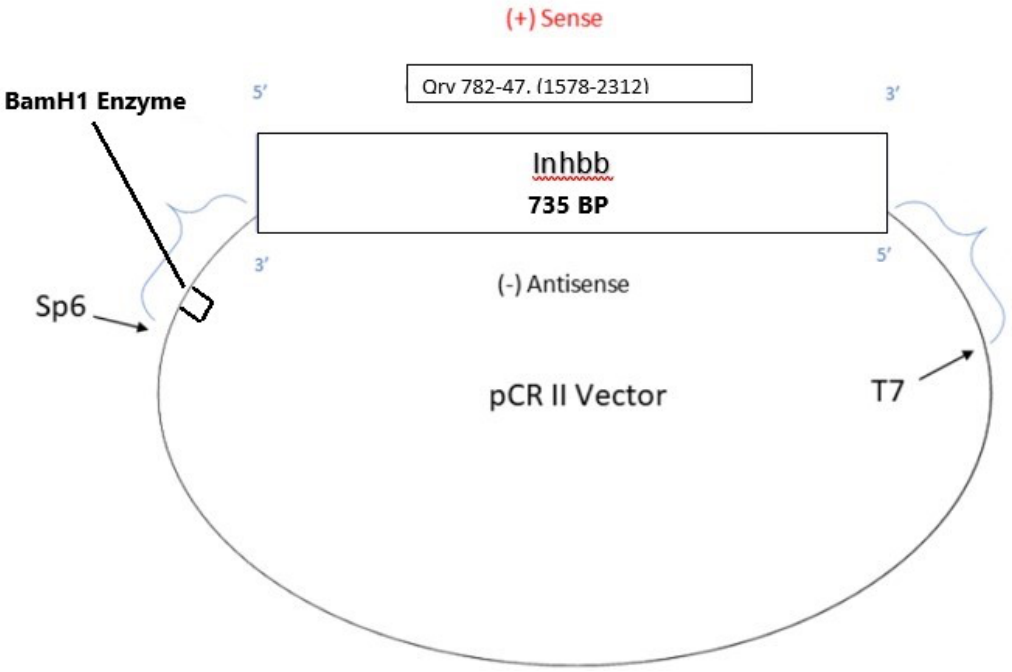


**Figure 8.** *Inhbb* pCR™II vector map. The base pair length, orientation, location of forward and reverse primers, and BamH1 enzyme location is shown.

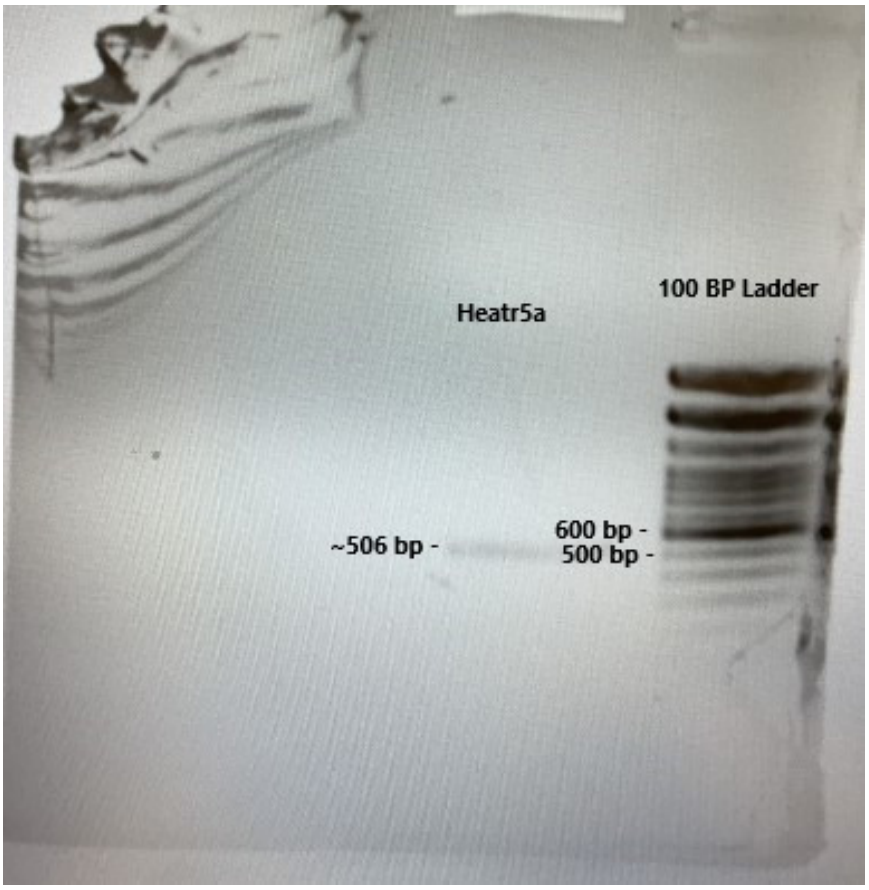


**Figure 9.** Gel electrophoresis product of *Heatr5a* PCR sublcone compared to a 100 BP Ladder. Band size showed a positive result of 506 base pairs which confirmed our product was the correct sequence length. This PCR product was then ligated with TA-cloning pCR™II vector.

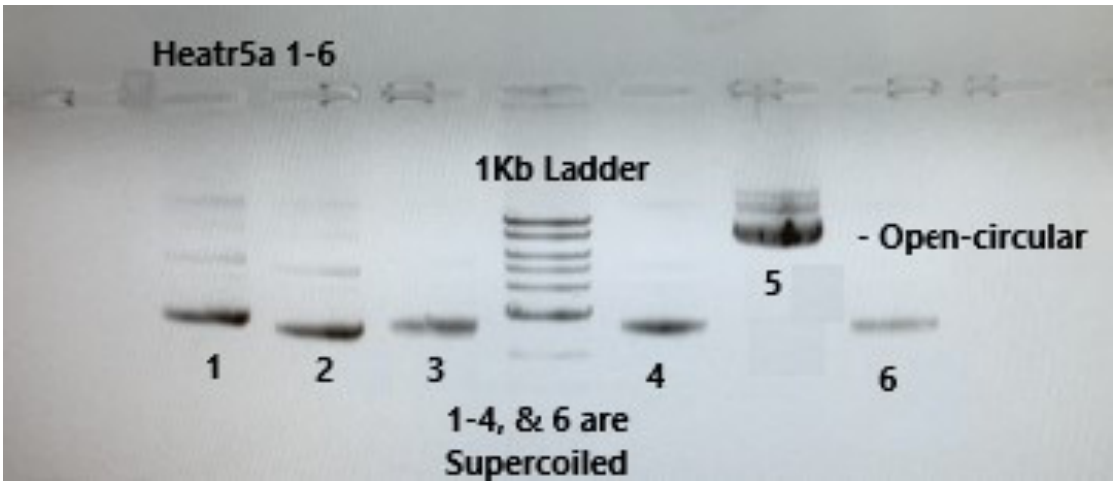


**Figure 10.** Gel electrophoresis product of *Heatr5a* that has been grown up in a liquid culture and purified. The band length is compared to a 1Kb BP Ladder and is just under 3Kb BP in length which confirms our product is the correct length. This is considering the dark staining to be a supercoiled version of the plasmid vector (1-4, & 6). The 5$^{th}$ row is considered to be in the open circular orientation. This product was sent off for sequencing (GeneWiz).

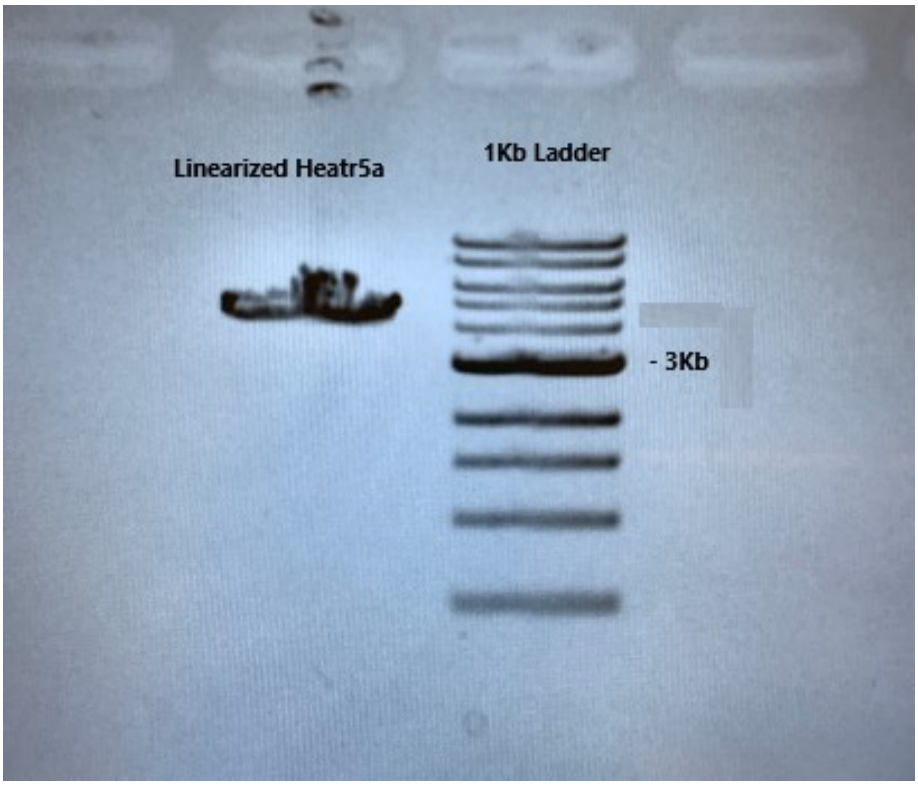


**Figure 11.** Gel electrophoresis product of purified *Heatr5a* plasmid vector that has been linearized with BamH1. This product is compared with a 1Kb BP Ladder and confirms the phenol/chloroform/isoamyl alcohol extraction was succesful. This product was used to make the final riboprode product by adding a DIG labeling mixture to it.

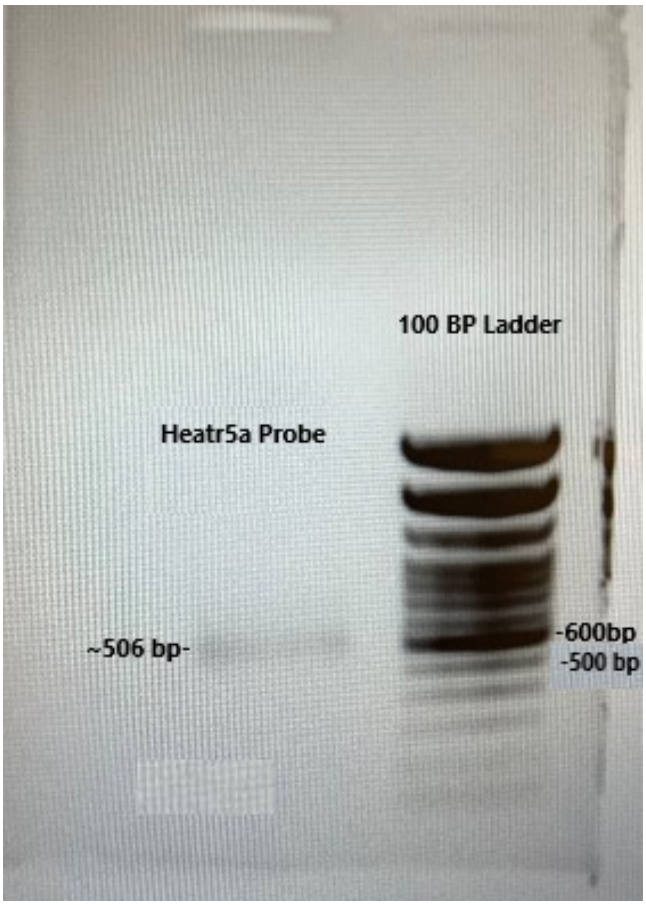


**Figured 12.** Gel electrophoresis product of *Heatr5a* DIG labeled riboprobe compared to a 100 BP Ladder. The band size of 506 base pairs confirms that our sequence is of the right length. This product was used in our In-situ Hybridization experiments to show the expression of *Heatr5a* in both the transection-injured and sham surgery mice.

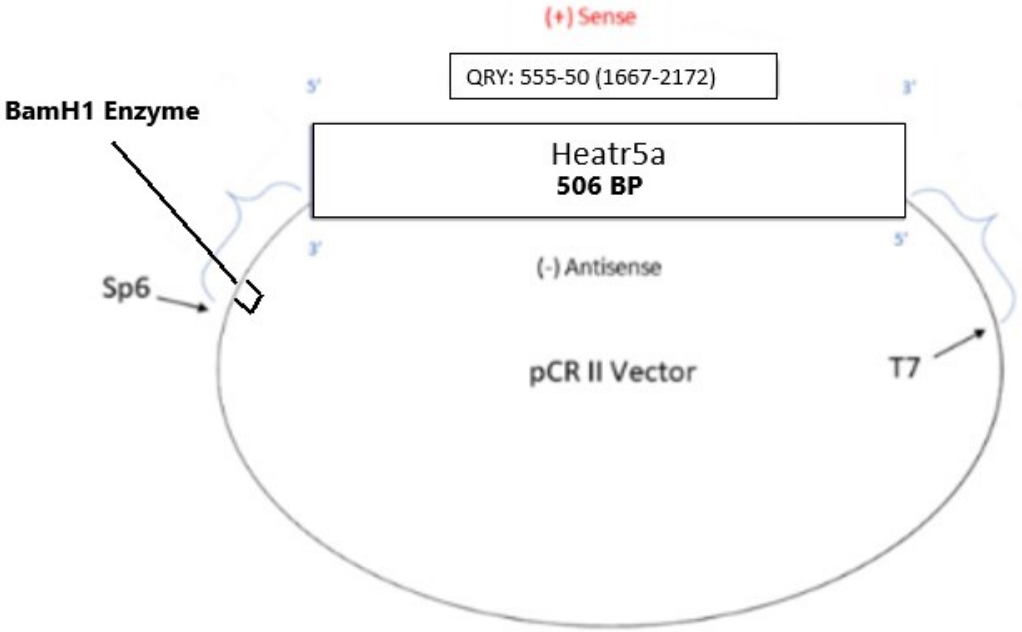


**Figure 13.** *Heatr5a* pCR™II vector map. The base pair length, orientation, location of forward and reverse primers, and BamH1 enzyme location is shown.

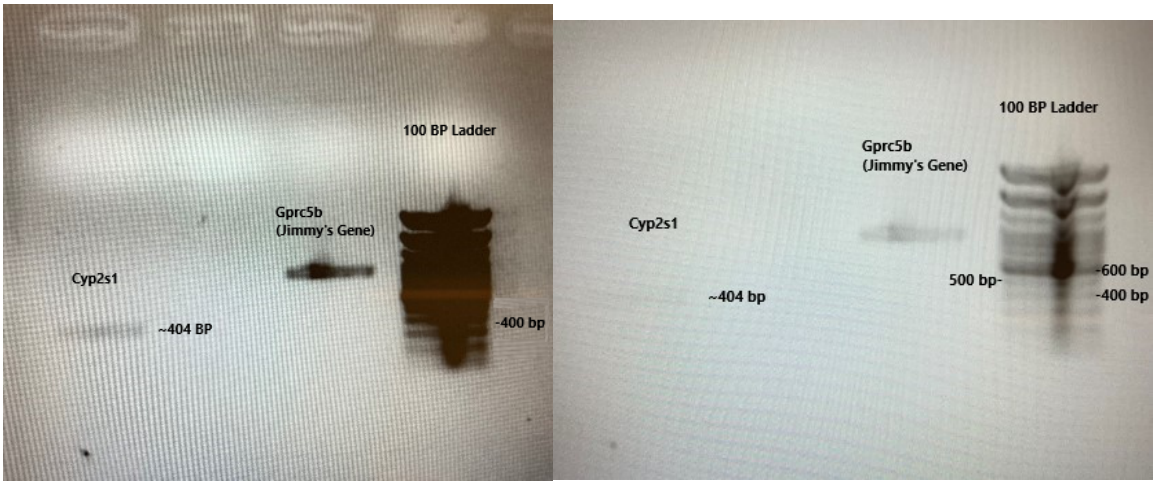


**Figure 14.** Gel electrophoresis product of *Cyp2s1* PCR sublcone compared to a 100 BP Ladder. Band size showed a positive result of 404 base pairs which confirmed our

product was the correct sequence length. This PCR product was then ligated with TA-cloning pCR™II vector.

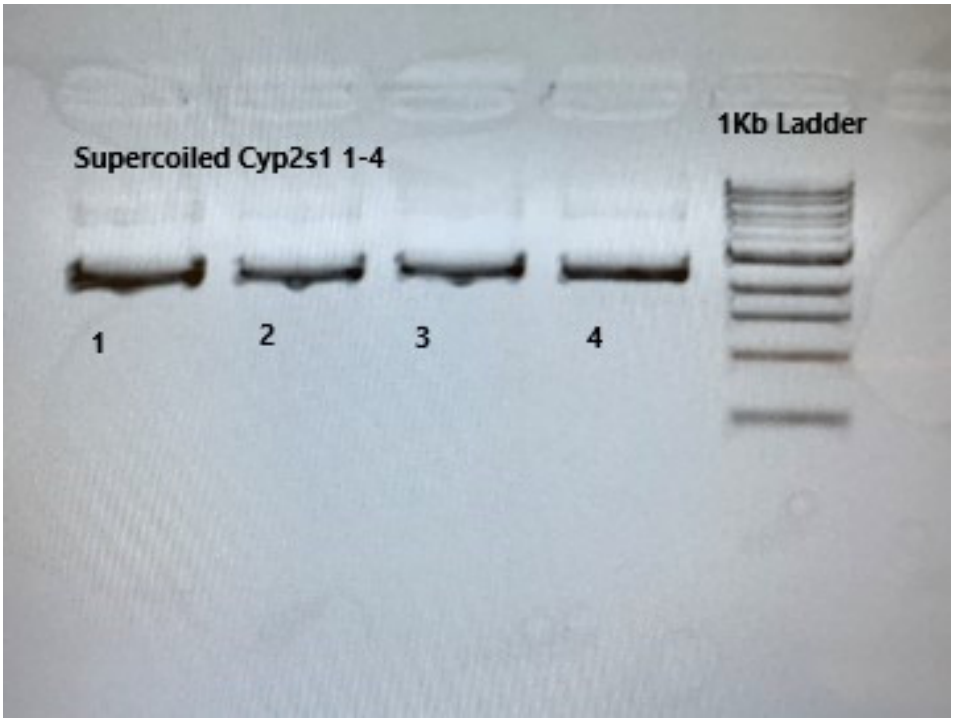


**Figure 15.** Gel electrophoresis product of *Cyp2s1* that has been grown up in a liquid culture and purified. The band length is compared to a 1Kb BP Ladder and is just under 3Kb BP in length which confirms our product is the correct length. This is considering the dark staining to be a supercoiled version of the plasmid vector. This product was sent off for sequencing (GeneWiz).

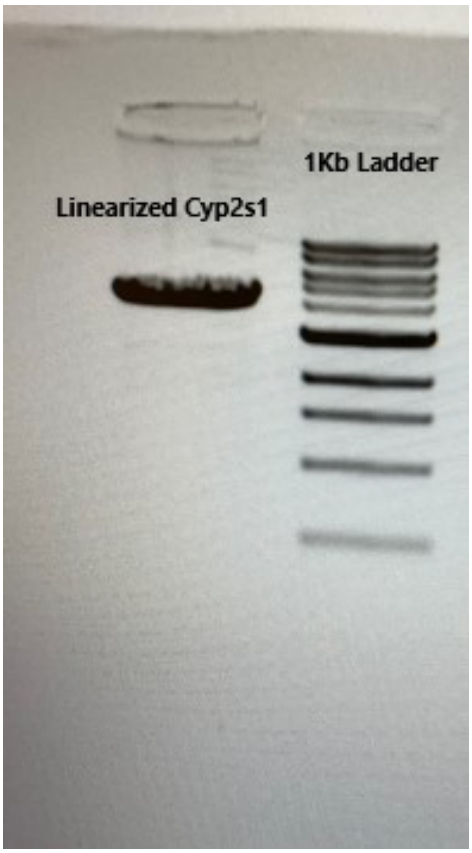


**Figure 16.** Gel electrophoresis product of purified *Cyp2s1* plasmid vector that has been linearized with XhoI. This product is compared with a 1Kb BP Ladder and confirms the phenol/chloroform/isoamyl alcohol extraction was succesful. This product was used to make the final riboprode product by adding a DIG labeling mixture to it.

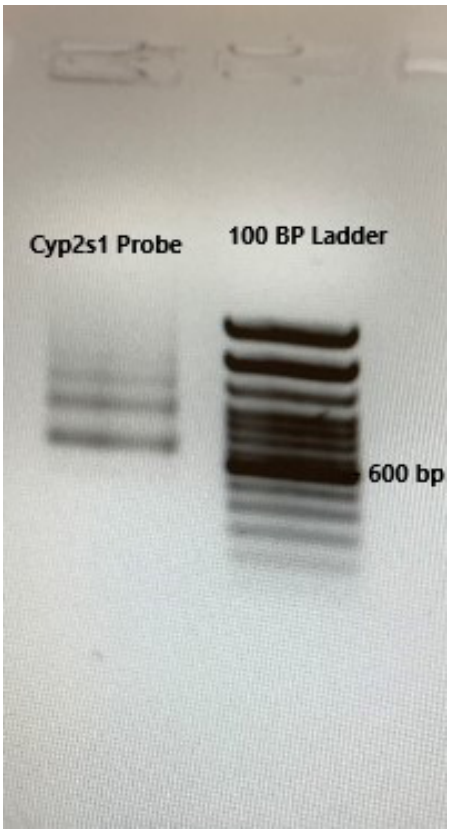


**Figure 17.** Gel electrophoresis product of *Cyp2s1* DIG labeled riboprobe compared to a 100 BP Ladder. The band size of above 600 base pairs does not confirm that our sequence is of the right length. However, our product was sequenced previously with GeneWiz, and due to time constraint we decided to proceed. This product was used in our In-situ Hybridization experiments to show the expression of *Cyp2s1* in both the transection-injured and sham surgery mice.

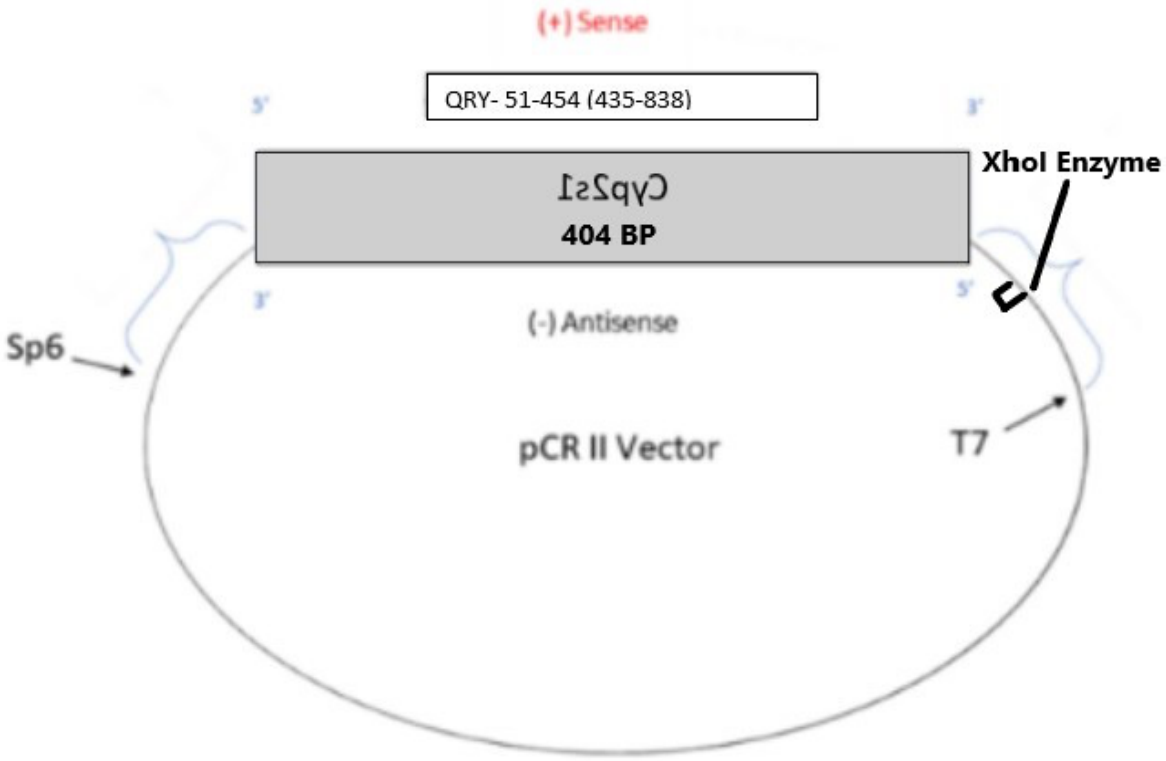


**Figure 18.** *Cyp2s1* pCR™II vector map. The base pair length, orientation, location of forward and reverse primers, and XhoI enzyme location is shown.

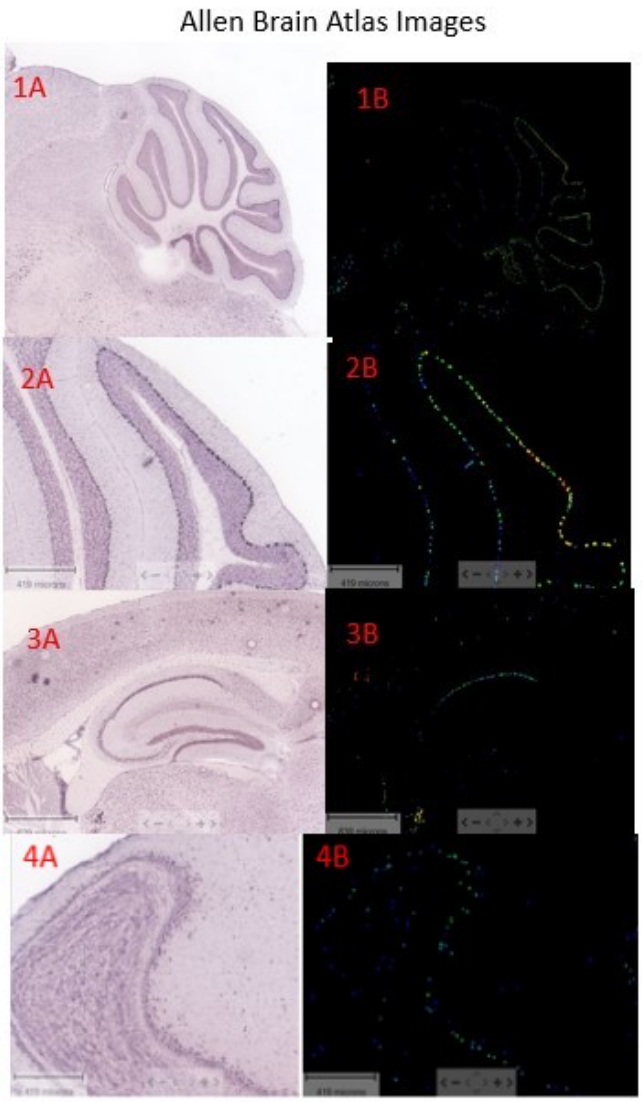


**Figure 19.** In-situ Hybridization results of *Inhbb* expression in a mouse brain (Allen, 2007). 1A/2A: Expression of *Inhbb* in the cerebellum. 1B/2B: ABA look up table expression of *Inhbb* from 1A & 2A respectively. This expression is significant when compared to other regions of the brain tissue. 3A/3B: Expression of *Inhbb* in the hippocampus. This expression is significant when compared to other regions of the brain tissue. 4A/4B: Expression of *Inhbb* in the olfactory bulb. This expression is significant when compared to other regions of the brain tissue.

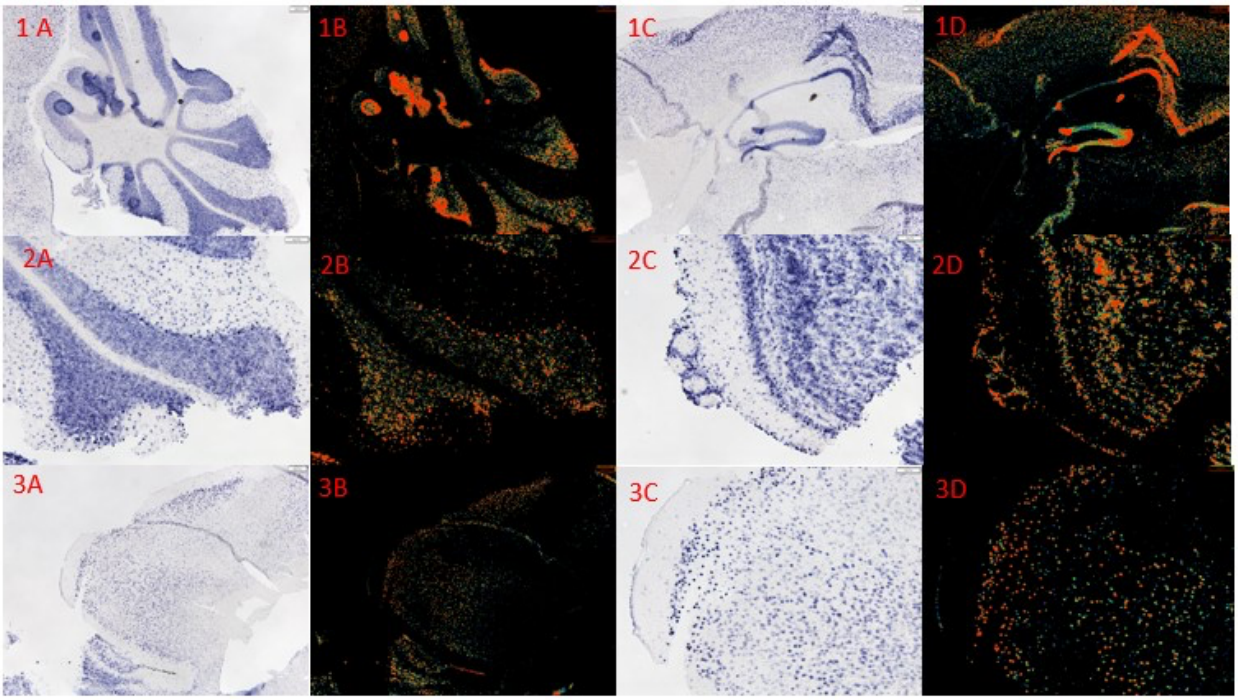


**Figure 20.** In-situ Hybridization results from *Inhbb* ribroprobe on brain tissue of a 93-week-old mouse. 1A/2A/1B/2B: Expression in the cerebellum. This staining was significant when compared to other tissue in the brain and also mirrors the *Inhbb* expression found in the ABA images. 3A/3B/3C/3D: Expression in the cortex. This staining was significant when compared to other tissue in the brain. 1C/1D: Expression in the hippocampus. This staining was significant when compared to other tissue in the brain and also mirrors the *Inhbb* expression found in the ABA images. 2C/2D: Expression in the olfactory bulb. This staining was significant when compared to other tissue in the brain and also mirrors the *Inhbb* expression found in the ABA images.

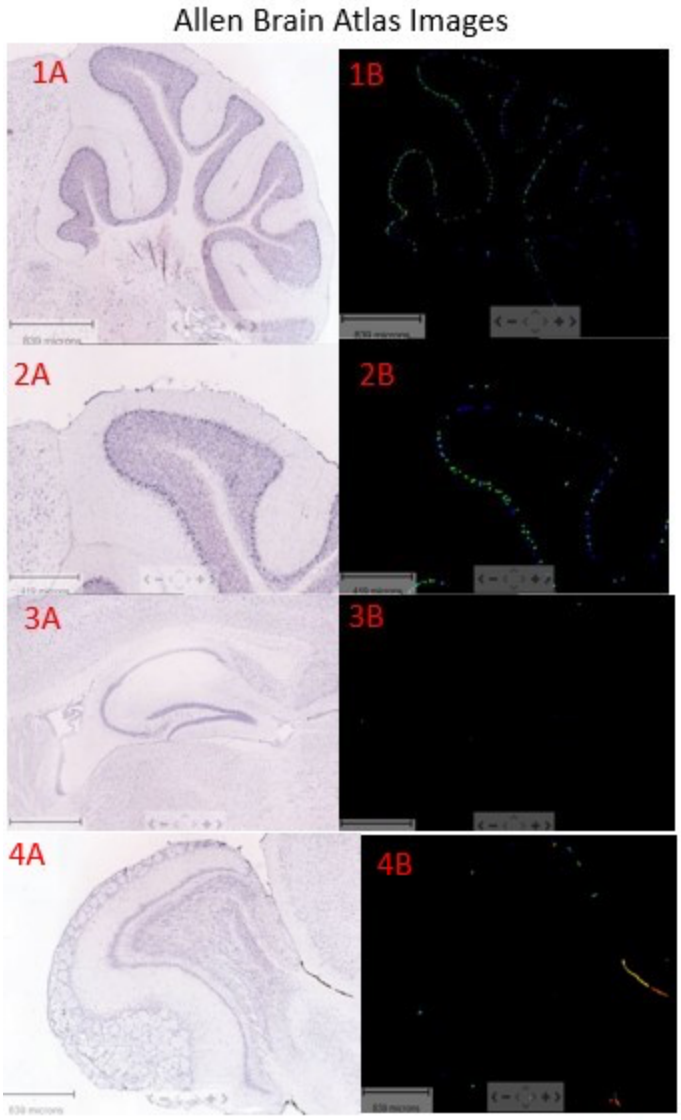


**Figure 21.** In-situ Hybridization results of *Heatr5a* expression in a mouse brain (Allen, 2007). 1A/2A: Expression of *Heatr5a* in the cerebellum. 1B/2B: ABA look up table expression of *Heatr5a* from 1A & 2A respectively. This expression is significant when compared to other regions of the brain tissue. 3A/3B: Expression of *Heatr5a* in the hippocampus. 4A/4B: Expression of *Heatr5a* in the olfactory bulb. This expression is significant when compared to other regions of the brain tissue. These images were taken

from the Allen Brain Atlas website and used as a tool to confirm proper expression of our control tissue (Allen, 2007).

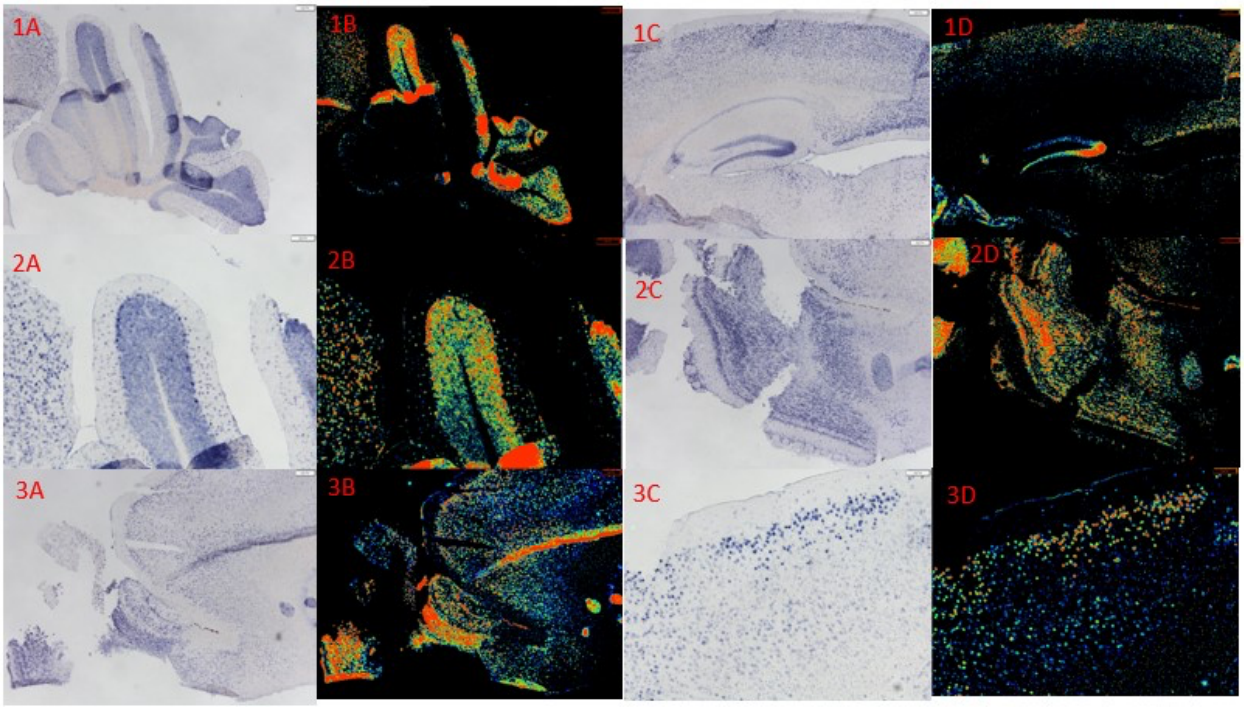


**Figure 22.** In-situ Hybridization results from *Heatr5a* ribroprobe on brain tissue of a 93-week-old mouse. 1A/2A/1B/2B: Expression in the cerebellum. This staining was significant when compared to other tissue in the brain and also mirrors the *Heatr5a* expression found in the ABA images. 3A/3B/3C/3D: Expression in the cortex. This staining was significant when compared to other tissue in the brain. 1C/1D: Expression in the hippocampus. 2C/2D: Expression in the olfactory bulb. This staining was significant when compared to other tissue in the brain and also mirrors the *Heatr5a* expression found in the ABA images.

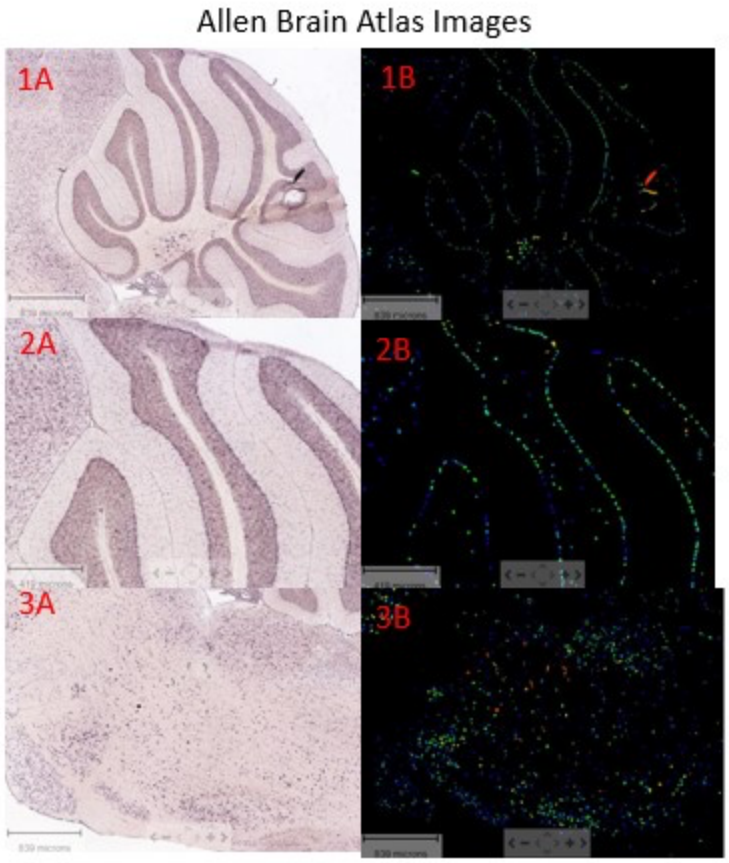


**Figure 23.** In-situ Hybridization results of *Cyp2s1* expression in a mouse brain (Allen, 2007). 1A/2A: Expression of *Cyp2s1* in the cerebellum. 1B/2B: ABA look up table expression of *Cyp2s1* from 1A & 2A respectively. This expression is significant when compared to other regions of the brain tissue. 3A/3B: Expression of *Cyp2s1* in the brain stem. This expression is significant when compared to other regions of the brain tissue, however expression for this gene in the brain stem was not tested. These images were taken from the Allen Brain Atlas website and used as a tool to confirm proper expression of our control tissue (Allen, 2007).

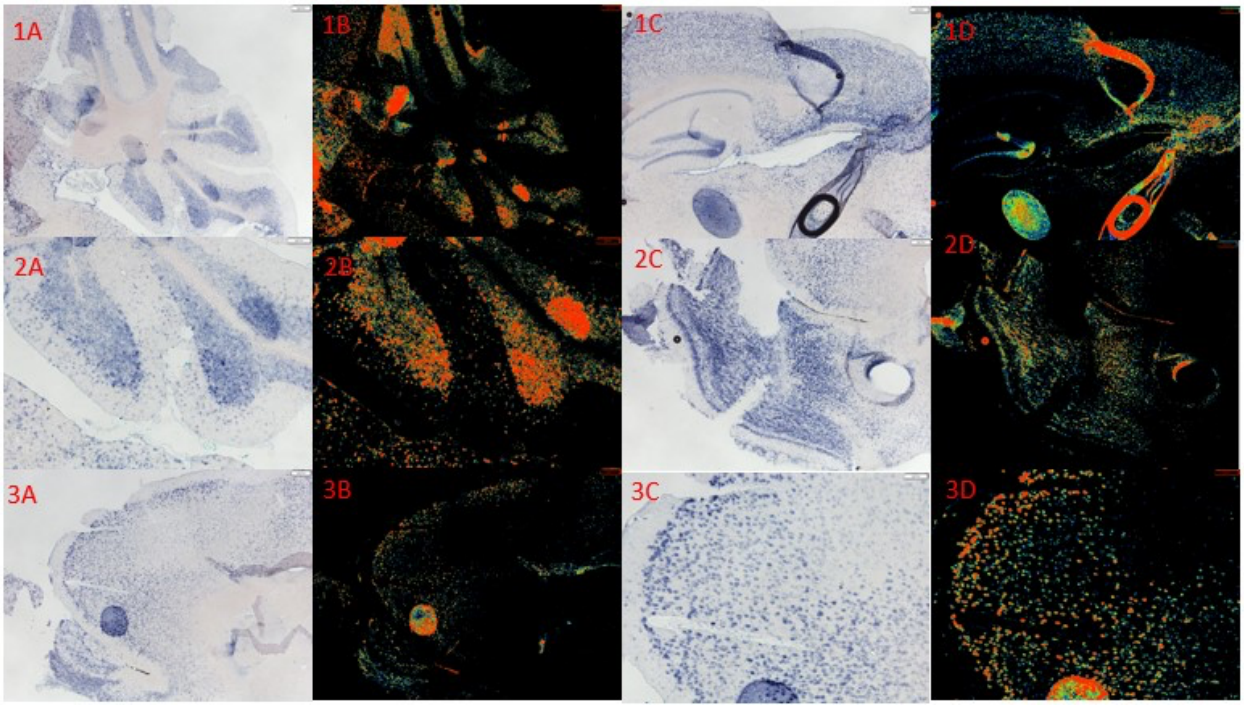


**Figure 24.** In-situ Hybridization results from *Cyp2s1* ribroprobe on brain tissue of a 93-week-old mouse. 1A/2A/1B/2B: Expression in the cerebellum. This staining was significant when compared to other tissue in the brain and also mirrors the *Cyp2s1* expression found in the ABA images. 3A/3B/3C/3D: Expression in the cortex. This staining was significant when compared to other tissue in the brain. 1C/1D: Expression in the hippocampus. 2C/2D: Expression in the olfactory bulb.

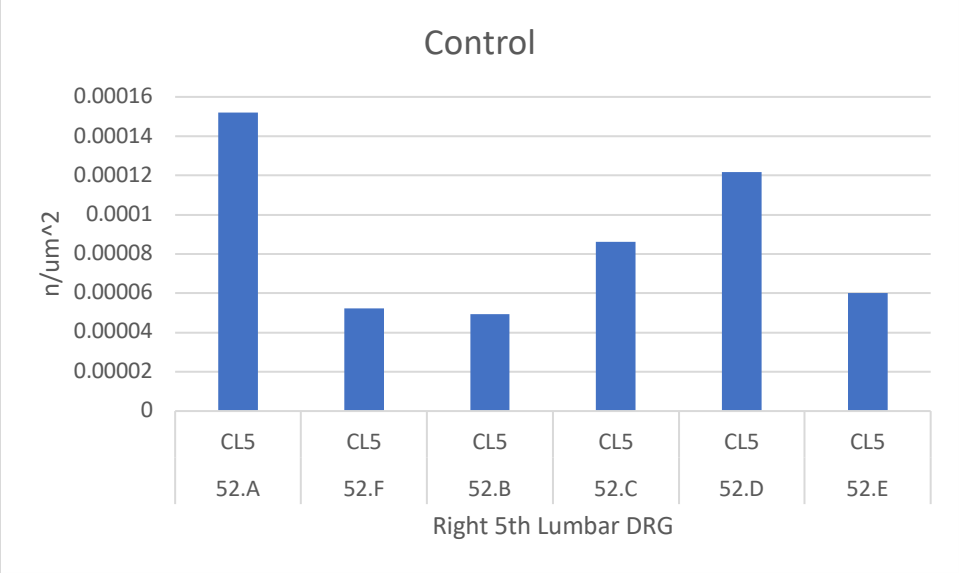


**Figure 25.** Comparing the number of genes expressed (dark staining) over the area of the total DRG in $\mu m^2$ in the Right $5^{th}$ Lumbar DRG for the *Inhbb* riboprobe. These figures showed the relationship between the sham injury animals and the transection-injured animals right L5 DRGs (nonaffected side). To calculate the specific area of each DRG, the ImageJ software was used and set to scale by measuring the 100 µm scale created by the CellSens software used to image the DRGs. Based on the data in this figure we observed no change in expression in our control tissues.

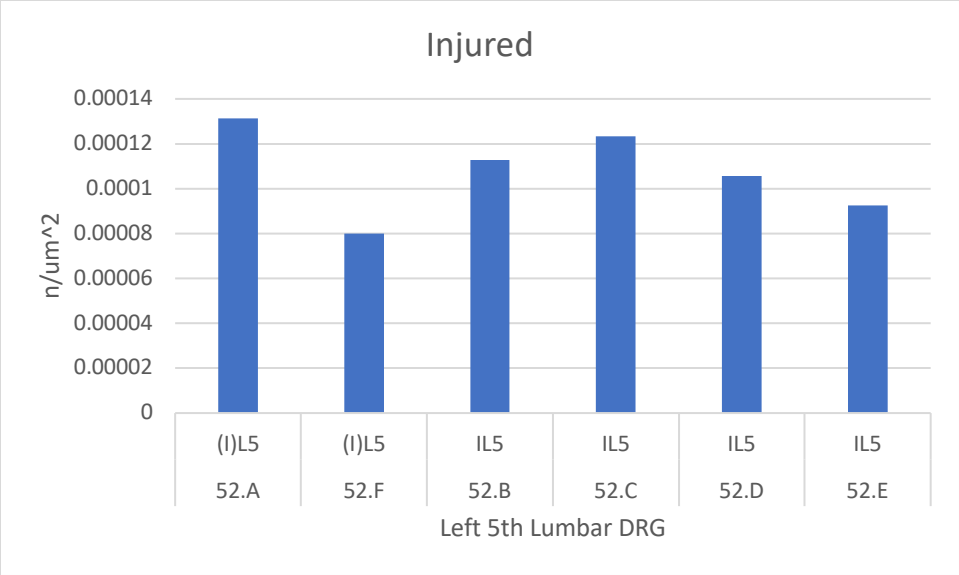


**Figure 26.** Comparing the number of genes expressed (dark staining) over the area of the total DRG in μm$^2$ in the Left 5$^{th}$ Lumbar DRG for the *Inhbb* riboprobe. These figures showed the relationship between the sham injury animals and the transection-injured animals Left L5 DRGs (affected side). To calculate the specific area of each DRG, the ImageJ software was used and set to scale by measuring the 100 μm scale created by the CellSens software used to image the DRGs. Based on the data in this figure we observed no change in our experimental tissue expression when compared to our control tissues.

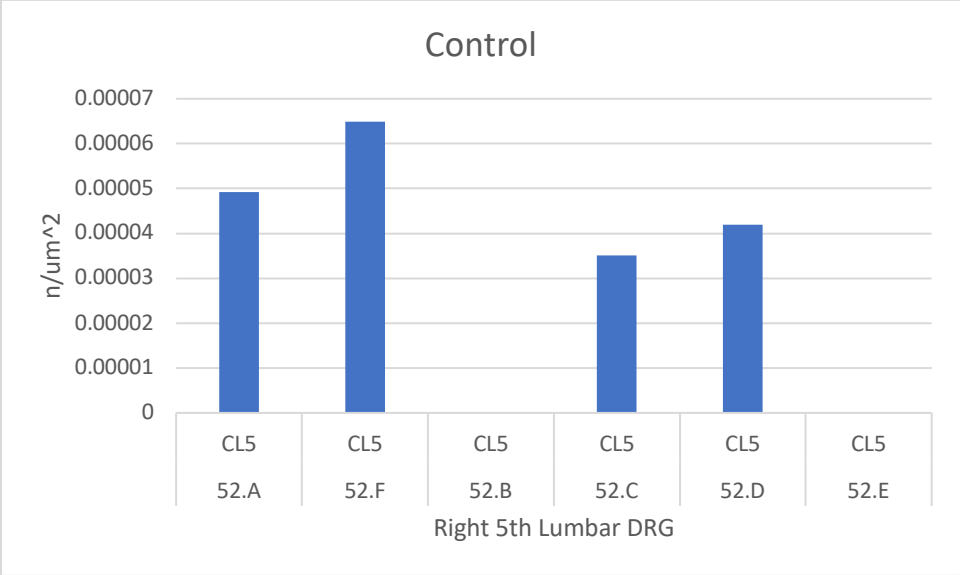


**Figure 27.** Comparing the number of genes expressed (dark staining) over the area of the total DRG in μm$^2$ in the Right 5$^{th}$ Lumbar DRG for the *Heatr5a* riboprobe. These figures showed the relationship between the sham injury animals and the transection-injured animals right L5 DRGs (nonaffected side). To calculate the specific area of each DRG, the ImageJ software was used and set to scale by measuring the 100 μm scale created by the CellSens software used to image the DRGs. Based on the data in this figure we observed no change in expression in our control tissues.

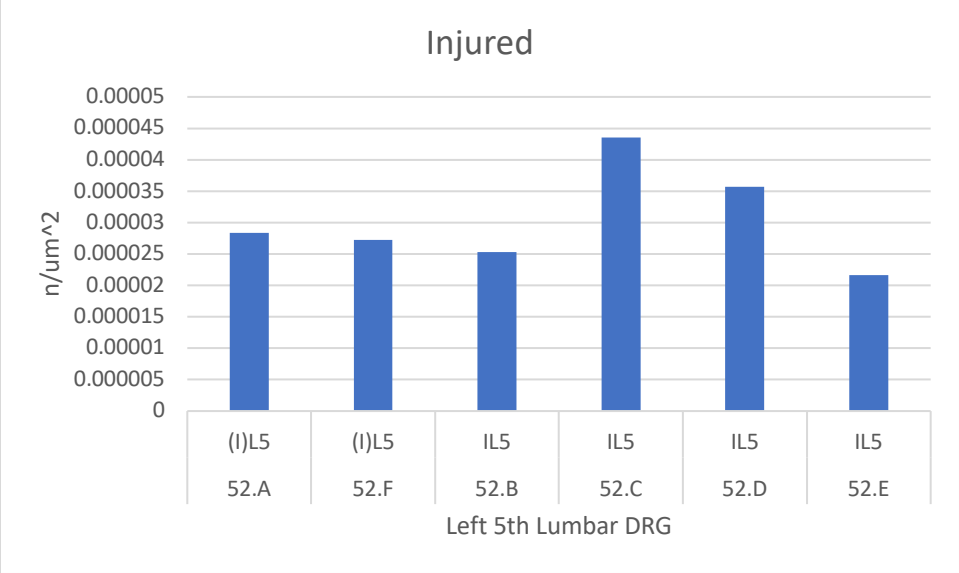


**Figure 28.** Comparing the number of genes expressed (dark staining) over the area of the total DRG in μm$^2$ in the Left 5$^{th}$ Lumbar DRG for the *Heatr5a* riboprobe. These figures showed the relationship between the sham injury animals and the transection-injured animals Left L5 DRGs (affected side). To calculate the specific area of each DRG, the ImageJ software was used and set to scale by measuring the 100 μm scale created by the CellSens software used to image the DRGs. Based on the data in this figure we observed no change in our experimental tissue expression when compared to our control tissues.

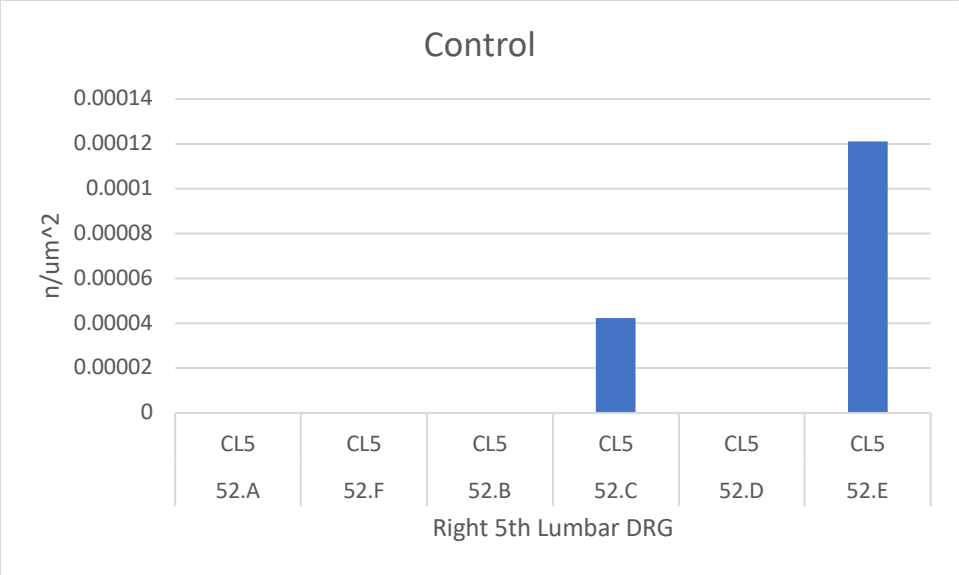


**Figure 29.** Comparing the number of genes expressed (dark staining) over the area of the total DRG in μm$^2$ in the Right 5$^{th}$ Lumbar DRG for the *Cyp2s1* riboprobe. These figures showed the relationship between the sham injury animals and the transection-injured animals right L5 DRGs (nonaffected side). To calculate the specific area of each DRG, the ImageJ software was used and set to scale by measuring the 100 μm scale created by the CellSens software used to image the DRGs. The data in this figure is inconclusive due to improper staining of the 52.A, 52.F, 52.B, and 52.D animals.

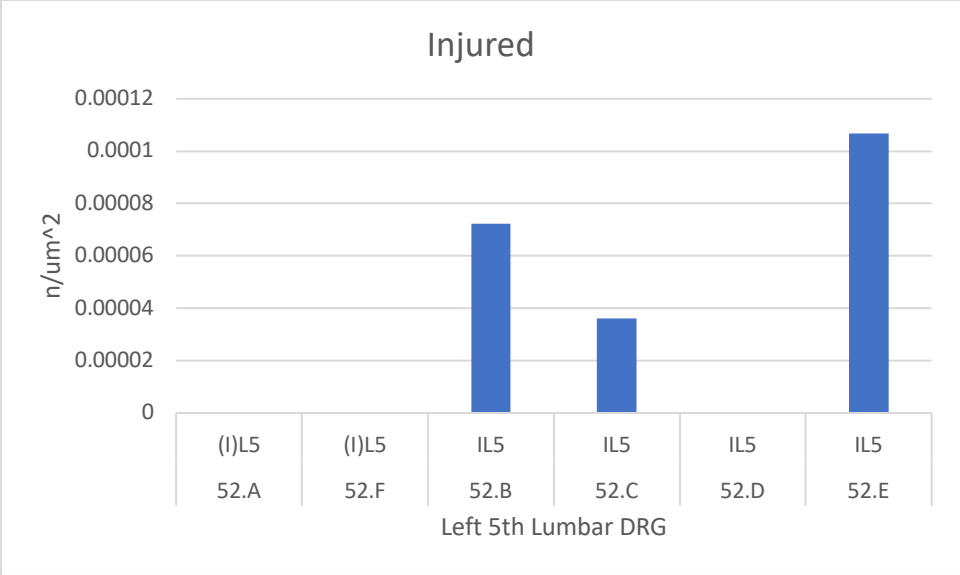


**Figure 30.** Comparing the number of genes expressed (dark staining) over the area of the total DRG in μm$^2$ in the Left 5$^{th}$ Lumbar DRG for the *Cyp2s1* riboprobe. These figures showed the relationship between the sham injury animals and the transection-injured animals Left L5 DRGs (affected side). To calculate the specific area of each DRG, the ImageJ software was used and set to scale by measuring the 100 μm scale created by the CellSens software used to image the DRGs. The data in this figure is inconclusive due to improper staining of the 52.A, 52.F, and 52.D animals.

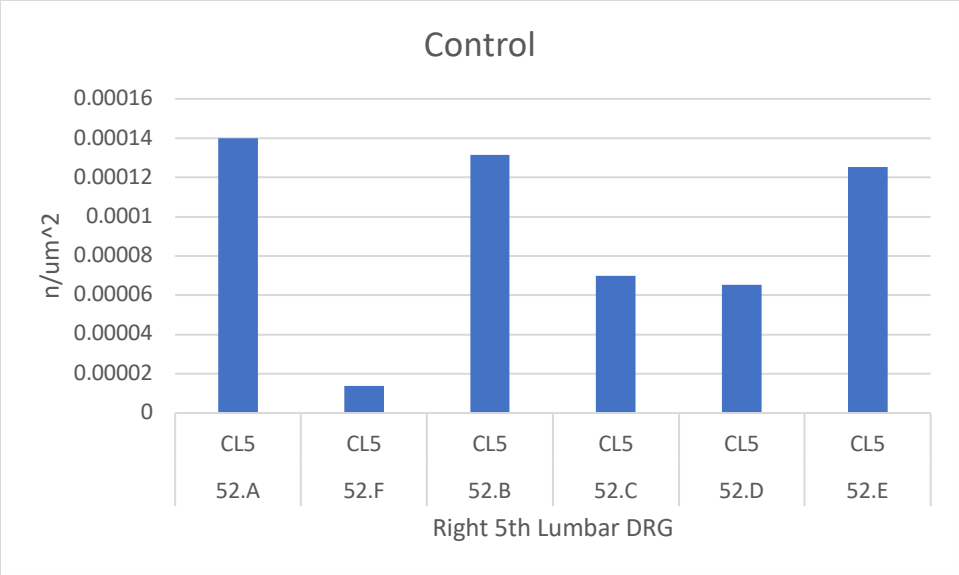


**Figure 31.** Comparing the number of genes expressed (dark staining) over the area of the total DRG in μm$^2$ in the Right 5$^{th}$ Lumbar DRG for the *PValb* riboprobe. These figures showed the relationship between the sham injury animals and the transection-injured animals right L5 DRGs (nonaffected side). To calculate the specific area of each DRG, the ImageJ software was used and set to scale by measuring the 100 μm scale created by the CellSens software used to image the DRGs. Based on the data in this figures we observed no change in expression in our control tissues.

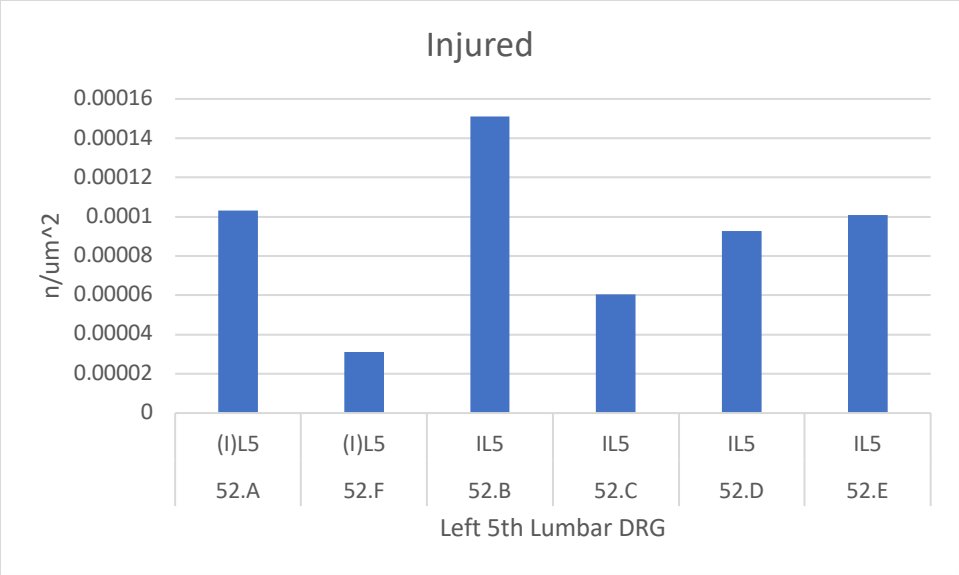


**Figure 32.** Comparing the number of genes expressed (dark staining) over the area of the total DRG in μm$^2$ in the Left 5$^{th}$ Lumbar DRG for the *PValb* riboprobe. These figures showed the relationship between the sham injury animals and the transection-injured animals Left L5 DRGs (affected side). To calculate the specific area of each DRG, the ImageJ software was used and set to scale by measuring the 100 μm scale created by the CellSens software used to image the DRGs. Based on the data in this figure we observed no change in our experimental tissue expression when compared to our control tissues.

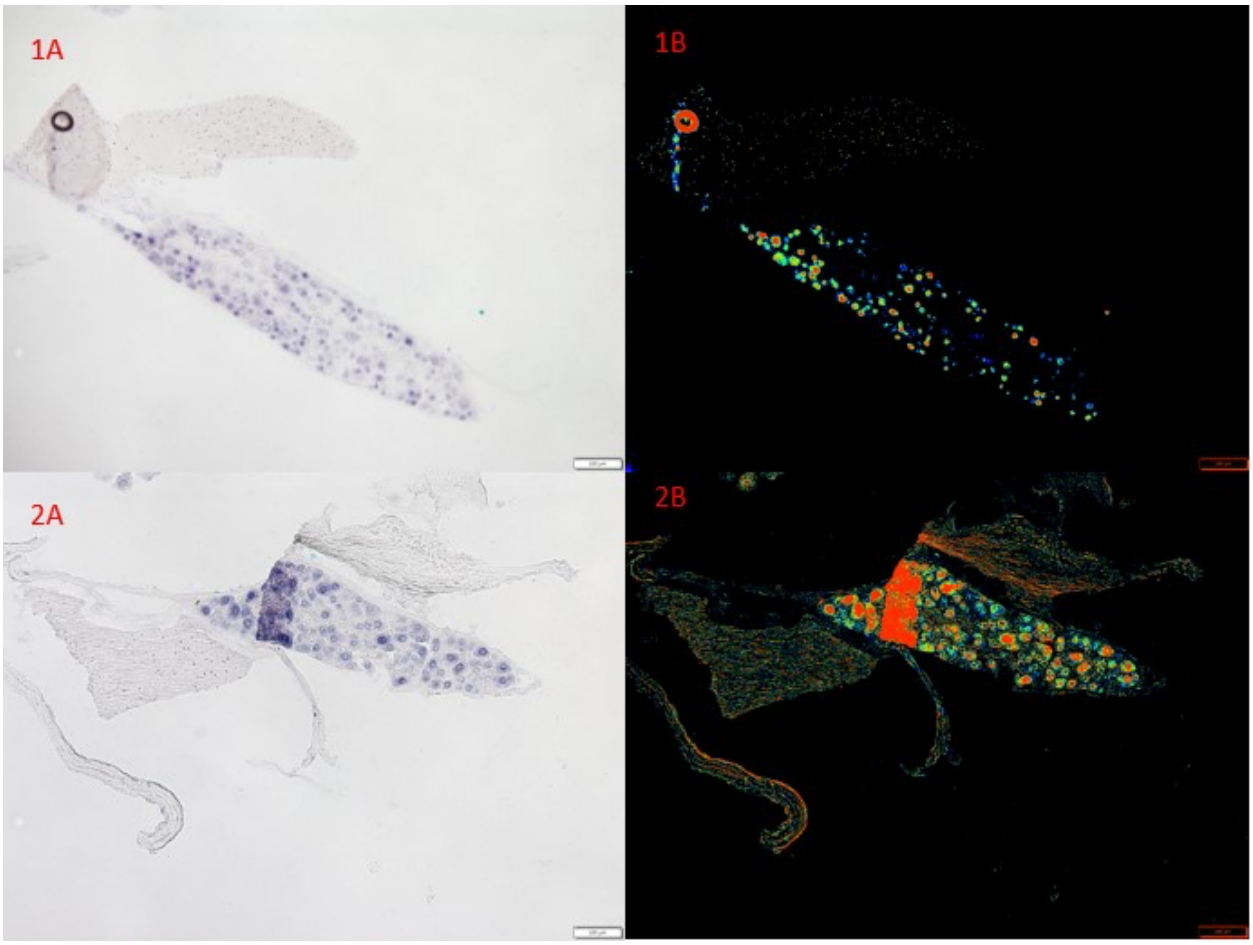


**Figure 33.** 1A/1B: Expression of *Inhbb* in a Right L5 DRG from a sham animal (Control). 2A/2B: Expression of *Inhbb* in a Left L5 DRG from a sham animal (Control). Scale bar equals 100 µm.

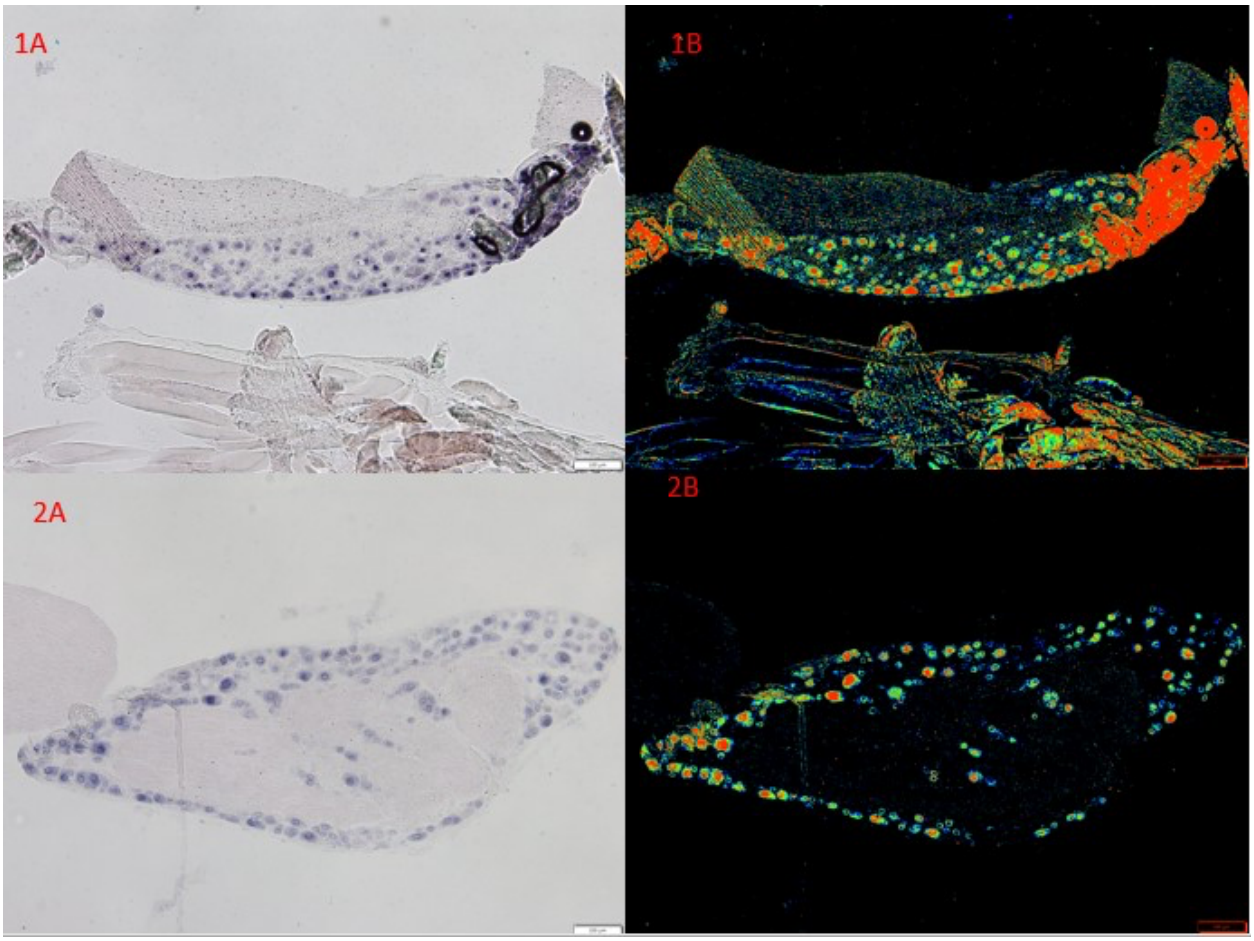


**Figure 34.** 1A/1B: Expression of *Inhbb* in a Right L5 DRG from a transection-injured animal (Control). 2A/2B: Expression of *Inhbb* in a Left L5 DRG from a transection-injured animal. Scale bar equals 100 µm.

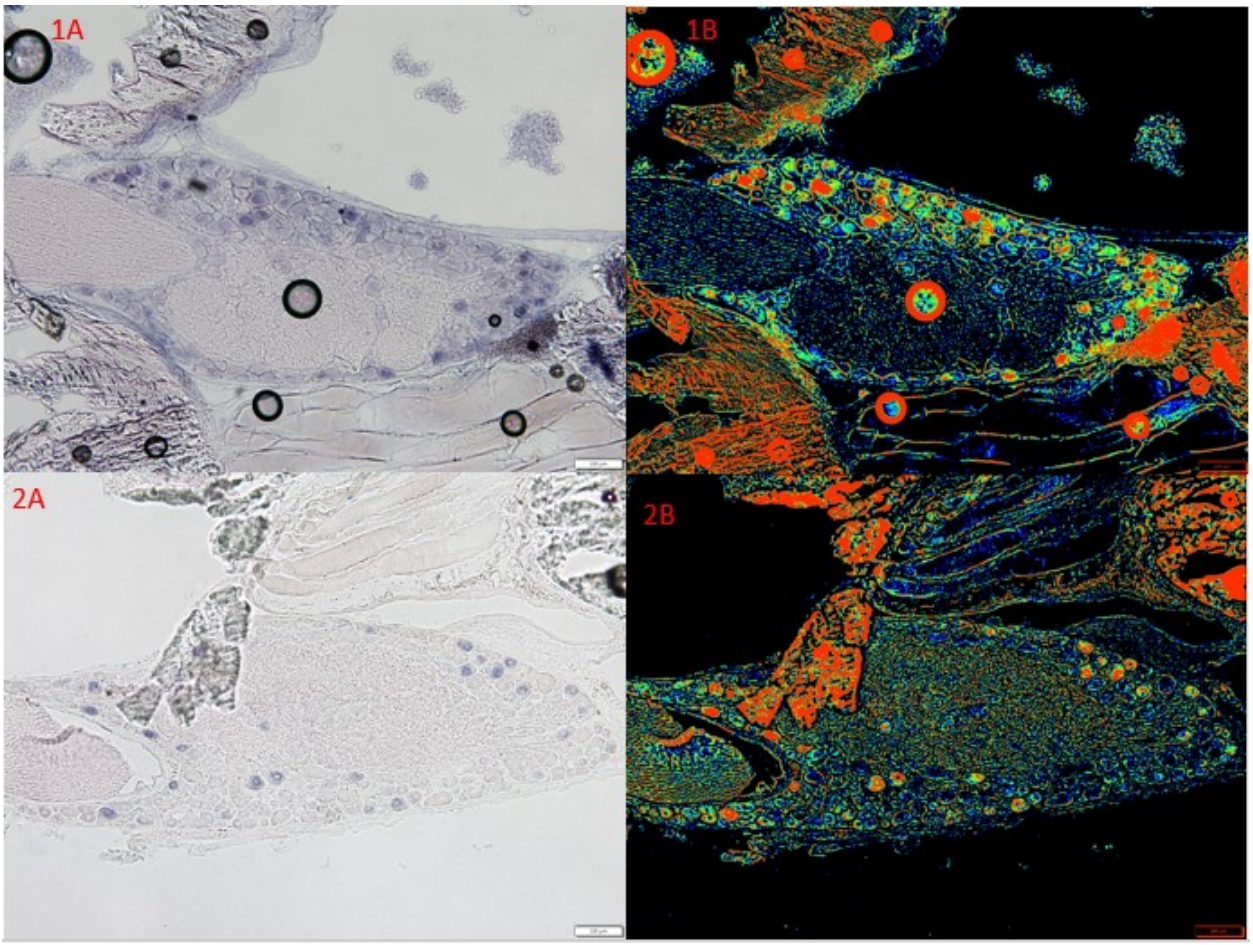


**Figure 35.** 1A/1B: Expression of *Heatr5a* in a Right L5 DRG from a sham animal (Control). 2A/2B: Expression of *Heatr5a* in a Left L5 DRG from a sham animal (Control). Scale bar equals 100 µm.

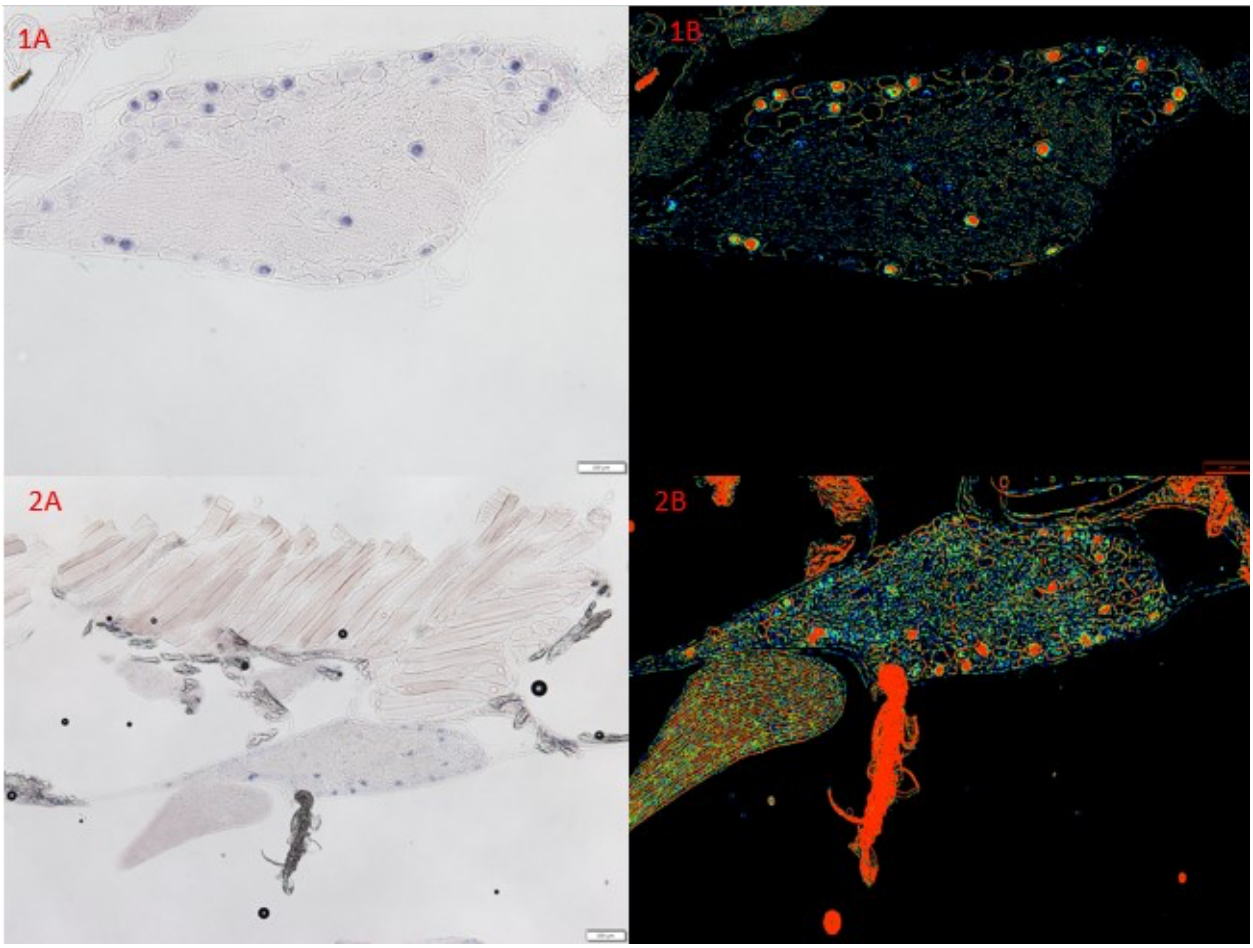


**Figure 36.** 1A/1B: Expression of *Heatr5a* in a Right L5 DRG from a transection-injured animal (Control). 2A/2B: Expression of *Heatr5a* in a Left L5 DRG from a transection-injured animal. Scale bar equals 100 µm.

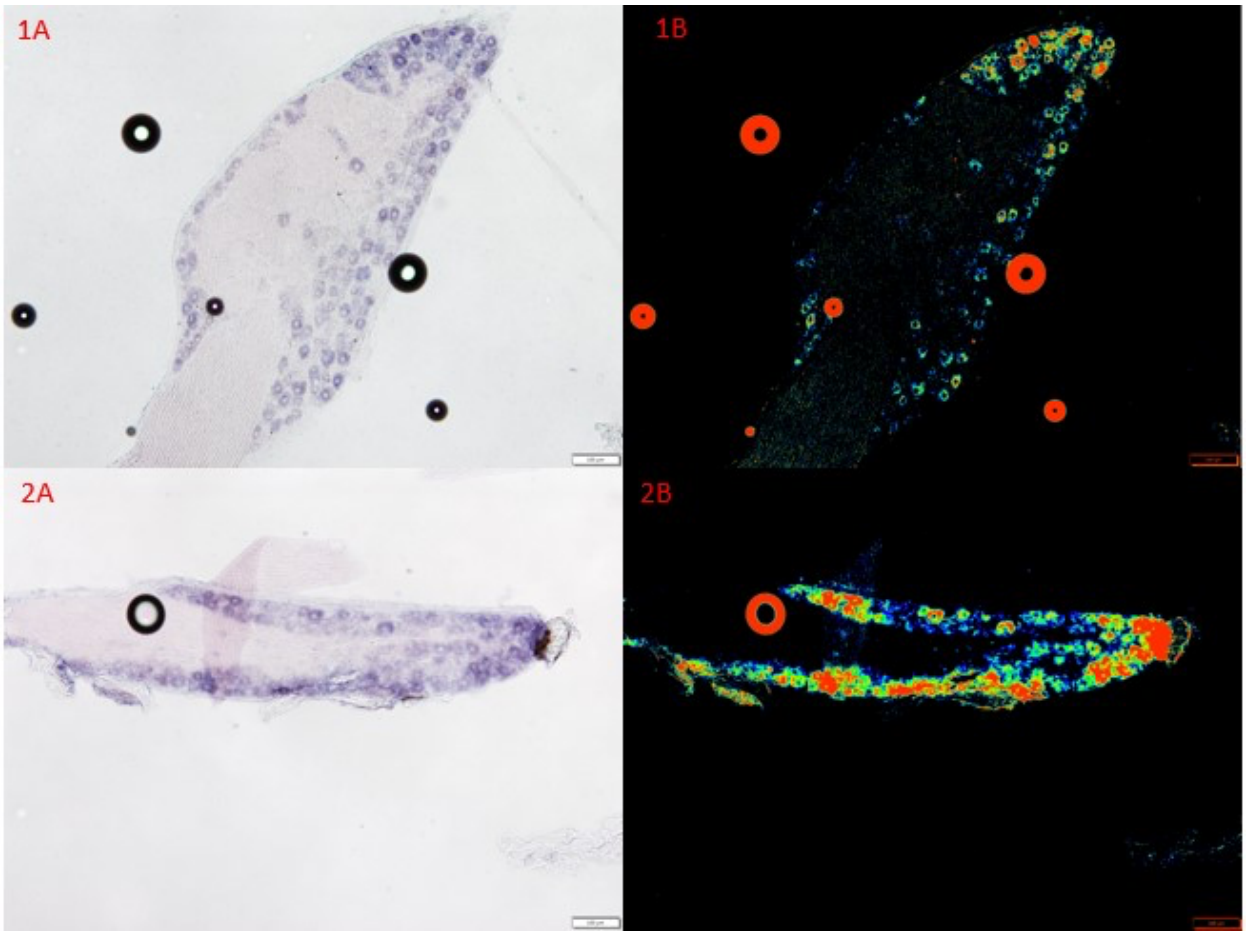


**Figure 37.** 1A/1B: Expression of *Cyp2s1* in a Right L5 DRG from a sham animal (Control). 2A/2B: Expression of *Cyp2s1* in a Left L5 DRG from a sham animal (Control). Scale bar equals 100 µm.

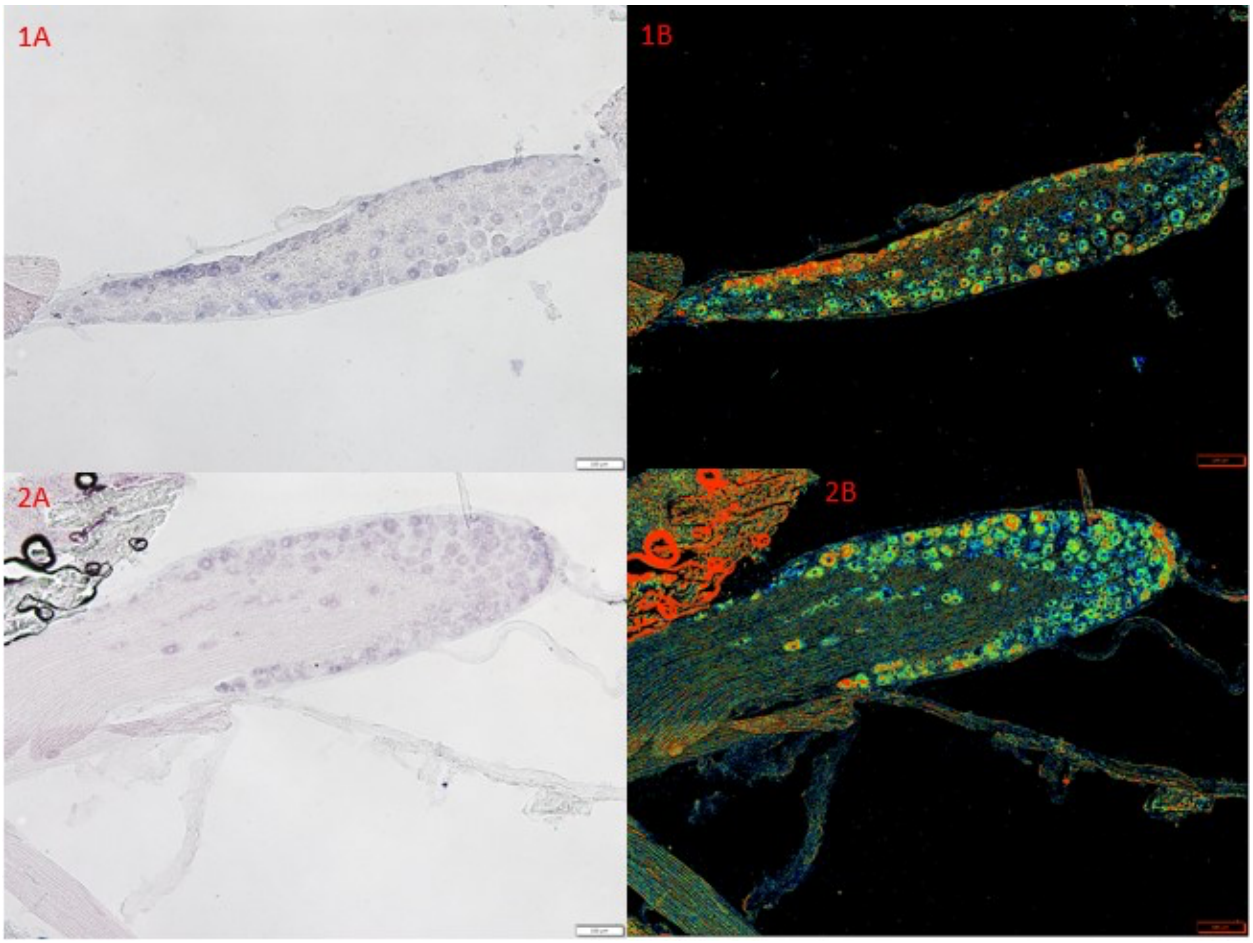


**Figure 38.** 1A/1B: Expression of *Cyp2s1* in a Right L5 DRG from a transection-injured animal (Control). 2A/2B: Expression of *Cyp2s1* in a Left L5 DRG from a transection-injured animal. Scale bar equals 100 µm.

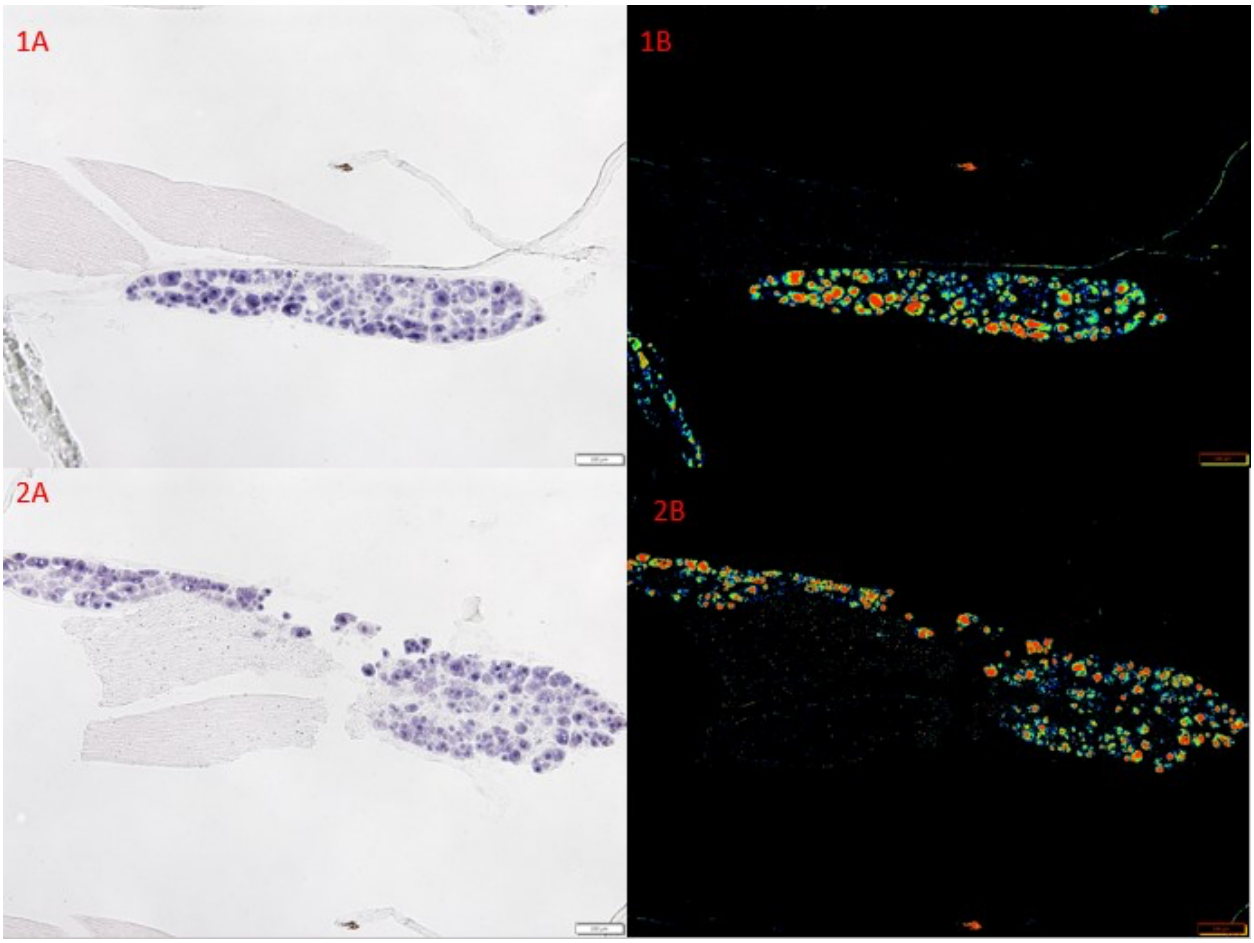


**Figure 39.** 1A/1B: Expression of *PValb* in a Right L5 DRG from a sham animal (Control). 2A/2B: Expression of *PValb* in a Left L5 DRG from a sham animal (Control). Scale bar equals 100 μm.

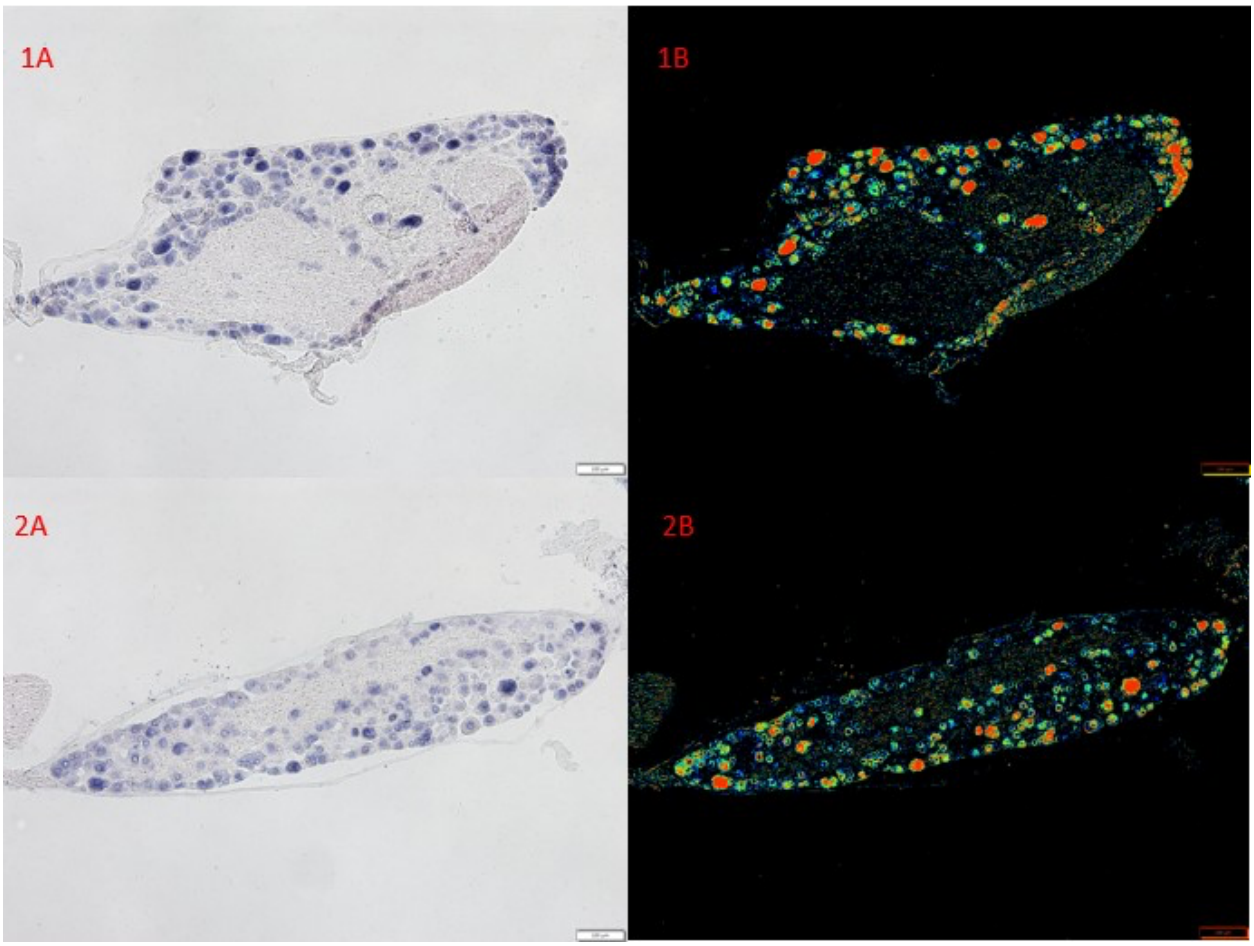


**Figure 40.** 1A/1B: Expression of *Pvalb* in a Right L5 DRG from a transection-injured animal (Control). 2A/2B: Expression of *Pvalb* in a Left L5 DRG from a transection-injured animal. Scale bar equals 100 µm.

## IV. Discussion

This study reviewed the effects of DIG labeled riboprobes which were used to observe the expression of three late marker genes *Inhbb, Heatr5a, Cyp2s1* in PNI lumbar DRG tissue. The results shown in our experiments confirmed that these DIG labeled riboprobes can be used to identify expression patterns within the DRG that are specific to PSNs.

### *Inhbb*

Reviewing Figure 1 in comparison to Figure 4, we can confirm that our band length in Figure 4 is the same base pair length as our insert from Figure 1. This indicates that the PCR product shown is the ready for the ligation stage. After ligating with the pCR™II vector the plasmid is purified. Figure 5 confirms that our DNA insert within the pCR™II vector is the correct base pair length. This figure shows the plasmid vector in a supercoiled state, which is one of three states the plasmid vector can be oriented in within the Gel. The other two states are open-circular (observed in Figure 10) and linearized (observed in Figures 6, 11, & 16). The speed in which these states run through the gel are open circular, linearized, and supercoiled from slowest to fastest (Cole and Tellez, 2002). The linearized plasmid vector for *Inhbb* is confirmed in Figure 6. This indicates that the phenol/chloroform/isoamyl alcohol extraction worked, and the BamH1 enzyme was able to properly cut the *Inhbb* plasmid. The final RNA probe was confirmed to have the specific base pair length associated in Figure 1.

In-situ hybridization results with the *Inhbb* riboprobe confirmed that this RNA probe can be used to show the expression of *Inhbb* in PNI tissue. As shown in figures 33 & 34 the expression patterns of *Inhbb* seem to be very nuclear in orientation when compared to the other riboprobes such *Cyp2s1* which showed more of a cytoplasmic expression (Figures 37 & 38). Using the 9.A mouse brain tissue as a control confirmed that our expression patterns for *Inhbb* in the brain tissue (Figures 20) when compared to the ABA (Figure 19) examples is unique. The overall expression patterns in Inhbb did not seem to change between the transection-injury and control tissue. Further investigation of this gene's expression needs to be done prior to making any certain conclusions. Future studies can focus on the expression on *Inhbb* in other tissue as well as in different aged mice, comparing young, adolescent, and adult mice. By reviewing this gene expression in other tissue when can better understand the role this gene has within the body.

***Heatr5a***

As previously stated, all the DNA labeled riboprobes showed confirmation of showing the specific gene expression with the PNI tissue. *Heatr5a* just like *Inhbb* had each step in the probe making process confirmed by Gel electrophoresis when compared to the band length and the respective base pair ladder. These findings are shown in Figures 9, 10, 11, & 12. When observing the In-situ hybridization tissue showing expression for *Heatr5a* (Figures 22, 35, and 36) confirms the ability of use for the riboprobe. *Heatr5a* in Figure 22 also showed to match the brain tissue expression pattern found in the ABA images on Figure 21. As previously stated with *Inhbb* further investigation of *Heatr5a*'s expression is needed to make any conclusive findings.

***Cyp2s1***

*Cyp2s1* unlike the other genes had two slides 52.D and 52.F which did not show any expression within the DRGs. No evidence was shown during experimentation that would indicate this result. However, whether human error or improper band length shown in Figure 17 we at least met our first goal of creating a riboprobe which expression specific signaling in DRG tissue. All the steps in the probe making processed were confirmed with Gels as shown in Figures 14, 15, and 16. As stated previously the purified plasmid was sent for sequencing, so we knew our final product had our unique sequence, but do not know why this was not represented in Figure 17. However, the brain tissue signaling (Figure 24) still matched the expression shown in the ABA (Figure 23) tissue. When looking at Figures 37 and 38 a unique cytoplasmic expression is shown which is different compared to the other gene expressions. Further investigation could help answer the questions revealed in this study. For example, why did the late marker gene expression patterns not differ from the control and injured tissue? Originally, we hypothesized that since these peripheral nerves are in a regenerative state that they would express an increase in early embryonic markers and a decrease in late markers. However, due to time constraints we were not able to observe expression patterns with any early markers. Creating new riboprobes specific for early embryonic markers would be needed to further explain this question. Technical improvements, such as revising mounting techniques as well as other practices are needed to observe more crisp data. This includes increasing the sample size, observing gene expression before and after injury, and testing these probes on various ages of mice.

## V. References


Allen. (2007). ALLEN Mouse Brain Atlas. Gene Expression. https://doi.org/10.1038/nature05453

Banks RW, Barker D (1989) Specificities of afferents reinnervating cat muscle spindles after nerve section. J Physiol.

Beirowski B, Adalbert R, Wagner D, Grumme DS, Addicks K, Ribchester RR, Coleman MP (2005) The progressive nature of Wallerian degeneration in wild-type and slow Wallerian degeneration (WldS) nerves. BMC Neurosci.

Bullinger KL, Nardelli P, Pinter MJ, Alvarez FJ, Cope TC (2011) Permanent central synaptic disconnection of proprioceptors after nerve injury and regeneration. II. Loss of functional connectivity with motoneurons. J Neurophysiol.

Chaudhry V, Cornblath DR (1992) Wallerian degeneration in human nerves: Serial electrophysiological studies. Muscle Nerve.

Chen P, Piao X, Bonaldo P (2015) Role of macrophages in Wallerian degeneration and axonal regeneration after peripheral nerve injury. Acta Neuropathol.

Cole, K. D., & Tellez, C. M. (2002). Separation of large circular DNA by electrophoresis in agarose gels. Biotechnology progress, 18(1), 82-87.

Collins WF, Mendell LM, Munson JB (1986) On the specificity of sensory reinnervation of cat skeletal muscle. J Physiol.

Elzinga K, Tyreman N, Ladak A, Savaryn B, Olson J, Gordon T (2015) Brief electrical stimulation improves nerve regeneration after delayed repair in Sprague Dawley rats. Exp

Neurol.

Fu SY, Gordon T (1997) The cellular and molecular basis of peripheral nerve regeneration. Mol Neurobiol.

Gaudet AD, Popovich PG, Ramer MS (2011) Wallerian degeneration: Gaining perspective on inflammatory events after peripheral nerve injury. J Neuroinflammation.

George, E. B., Glass, J. D., & Griffin, J. W. (1995). Axotomy-induced axonal degeneration is mediated by calcium influx through ion-specific channels. Journal of Neuroscience. https://doi.org/10.1523/jneurosci.15-10-06445.1995

Gordon T, English AW (2016) Strategies to promote peripheral nerve regeneration: Electrical stimulation and/or exercise. Eur J Neurosci.

Haftel VK, Bichler EK, Wang QB, Prather JF, Pinter MJ, Cope TC (2005) Central suppression of regenerated proprioceptive afferents. J Neurosci.

Hyde D, Scott JJA (1983) Responses of cat peroneus brevis muscle spindle afferents during recovery from nerve-crush injury. J Neurophysiol.

Kang H, Lichtman JW (2013) Motor axon regeneration and muscle reinnervation in young adult and aged animals. J Neurosci.

Komori N, Takemori N, Hee KK, Singh A, Hwang SH, Foreman RD, Chung K, Jin MC, Matsumoto H (2007) Proteomics study of neuropathic and nonneuropathic dorsal root ganglia: Altered protein regulation following segmental spinal nerve ligation injury. Physiol Genomics.

Kouyoumdjian, J. A. (2006). Peripheral nerve injuries: a retrospective survey of 456 cases.

Muscle & Nerve: Official Journal of the American Association of Electrodiagnostic Medicine, 34(6), 785-788.

Kouyoumdjian, J. A., Graça, C. R., & Ferreira, V. F. (2017). Peripheral nerve injuries: A retrospective survey of 1124 cases. Neurology India, 65(3), 551.

Kramer I, Sigrist M, De Nooij JC, Taniuchi I, Jessell TM, Arber S (2006) A role for Runx transcription factor signaling in dorsal root ganglion sensory neuron diversification. Neuron.

Lallemend F, Ernfors P (2012) Molecular interactions underlying the specification of sensory neurons. Trends Neurosci.

Levanon D, Bettoun D, Harris-Cerruti C, Woolf E, Negreanu V, Eilam R, Bernstein Y, Goldenberg D, Xiao C, Fliegauf M, Kremer E, Otto F, Brenner O, Lev-Tov A, Groner Y (2002) The Runx3 transcription factor regulates development and survival of TrkC dorsal root ganglia neurons. EMBO J.

Ma Q, Fode C, Guillemot F, Anderson DJ (1999) NEUROGENIN1 and NEUROGENIN2 control two distinct waves of neurogenesis in developing dorsal root ganglia. Genes Dev.

Missios, S., Bekelis, K., & Spinner, R. J. (2014). Traumatic peripheral nerve injuries in children: epidemiology and socioeconomics. Journal of Neurosurgery: Pediatrics, 14(6), 688-694.

Navarro, X., Vivó, M., & Valero-Cabré, A. (2007). Neural plasticity after peripheral nerve injury and regeneration. Progress in neurobiology, 82(4), 163-201.

Noble, J., Munro, C. A., Prasad, V. S., & Midha, R. (1998). Analysis of upper and lower extremity peripheral nerve injuries in a population of patients with multiple injuries. Journal of Trauma and Acute Care Surgery, 45(1), 116-122.

Pierrot-Deseilligny E, Morin C, Bergego C, Tankov N (1981) Pattern of group I fibre projections from ankle flexor and extensor muscles in man. Exp Brain Res.

Prather JF, Nardelli P, Nakanishi ST, Ross KT, Nichols TR, Pinter MJ, Cope TC (2011) Recovery of proprioceptive feedback from nerve crush. J Physiol.

Proske U, Gandevia SC (2012) The proprioceptive senses: Their roles in signaling body shape, body position and movement, and muscle force. Physiol Rev 92:1651–1697.

Raivich, G., & Makwana, M. (2007). The making of successful axonal regeneration: genes, molecules and signal transduction pathways. Brain research reviews, 53(2), 287-311.

Robinson, L. R. (2000). Traumatic injury to peripheral nerves. Muscle & Nerve: Official Journal of the American Association of Electrodiagnostic Medicine, *23*(6), 863-873.

Scheib J, Höke A (2013) Advances in peripheral nerve regeneration. Nat Rev Neurol.

Schultz AJ, Rotterman TM, Dwarakanath A, Alvarez FJ (2017) VGLUT1 synapses and P-boutons on regenerating motoneurons after nerve crush. J Comp Neurol.

Sunderland S (1947) Rate of regeneration of sensory nerve fibers. Arch Neurol Psychiatry.

Tsao JW, George EB, Griffin JW (1999) Temperature modulation reveals three distinct stages of Wallerian degeneration. J Neurosci.

Verdú E, Navarro X (1997) Comparison of immunohistochemical and functional reinnervation of skin and muscle after peripheral nerve injury. Exp Neurol.

Vincent JA, Nardelli P, Gabriel HM, Deardorff AS, Cope TC (2015) Complex impairment of IA muscle proprioceptors following traumatic or neurotoxic injury. J Anat.

Vogelaar CF, Vrinten DH, Hoekman MFM, Brakkee JH, Burbach JPH, Hamers FPT (2004) Sciatic nerve regeneration in mice and rats: Recovery of sensory innervation is followed by a slowly retreating neuropathic pain-like syndrome. Brain Res.

Wang Y, Wang H, Mi D, Gu X, Hu W (2015) Periodical assessment of electrophysiological recovery following sciatic nerve crush via surface stimulation in rats. Neurol Sci.

Wong JN, Olson JL, Morhart MJ, Chan KM (2015) Electrical stimulation enhances sensory recovery: A randomized controlled trial. Ann Neurol.

Wu D, Schieren I, Qian Y, Zhang C, Jessell TM, De Nooij JC (2019) A role for sensory end organ-derived signals in regulating muscle spindle proprioceptor phenotype. J Neurosci 39:4252–4267.

Zimny, M. L. (1988). Mechanoreceptors in articular tissues. American journal of anatomy, 182(1), 16-32.

Ziv, N. E., & Spira, M. E. (1993). Spatiotemporal distribution of Ca2+ following axotomy and throughout the recovery process of cultured Aplysia neurons. European Journal of Neuroscience, 5(6), 657-668.

Zuo J, Hernandez YJ, Muir D (1998) Chondroitin sulfate proteoglycan with neurite-inhibiting activity is up- regulated following peripheral nerve injury. J Neurobio.